Some Modeling and Optimization Problems in Cognitive Radio Ad Hoc Networks

Cunhao Gao

Thesis submitted to the Faculty of the
Virginia Polytechnic Institute and State University
in partial fulfillment of the requirements for the degree of

Master of Science
in
Computer Engineering

Y. Thomas Hou, Chair
Yi Shi
Yaling Yang

September 11, 2009
Blacksburg, Virginia

Keywords: Cognitive radio networks, multi-hop ad hoc network, optimization, multicast, resource allocation, MIMO, capacity

Some Modeling and Optimization Problems in Cognitive Radio Ad Hoc Networks

Cunhao Gao

ABSTRACT

Since its inception, cognitive radio (CR) has quickly been accepted as the enabling radio technology for next-generation wireless communications. A CR promises unprecedented flexibility in radio functionalities via programmability at the lowest layer, which was once done in hardware. Due to its spectrum sensing, learning, and adaptation capabilities, CR is able to address the heart of the problem associated with spectrum scarcity (via dynamic spectrum access (DSA)) and interoperability (via channel switching). It is envisioned that CR will be employed as a general radio platform upon which numerous wireless applications can be implemented.

For both theoretical and practical purposes, it is important for network researchers to model a cognitive radio ad hoc network (CRN) and optimize its performance. Such efforts are important not only for theoretical understanding, but also in that such results can be used as benchmarks for the design of distributed algorithms and protocols. However, due to some unique characteristics associated with CRNs, existing analytical techniques may not be applied directly. As a result, new theoretical results, along with new mathematical techniques, need to be developed. In this thesis, we focus on modeling and optimization of CRNs. In particular, we will study multicast communications in CRN and MIMO-empowered CRN, which we describe as follows.

An important service that must be supported by CRNs is multicast. Although there are a lot of research on multicast in ad hoc networks, those results cannot be applied to a CRN, because of the complexity associated with a CR node (e.g., multiple available frequency bands, difference in available bands from neighboring nodes). In addition, a single-layer approach (e.g., multicast routing) is overly simplistic when resource optimization (i.e., minimizing network resource) is the main objective. For this purpose, a cross-layer approach is usually necessary, which should include joint consideration of multiple lower layers, in addition to network layer. However, such a joint

formulation is usually highly complex and difficult. In this thesis, we aim to develop some novel algorithms that provide near-optimal solutions. Our goal is to minimize the required network-wide resource to support a set of multicast sessions, with a certain bit rate for each multicast session. The unique characteristics associated with CR and distinguish this problem from existing multicast research for ad hoc networks. In this work, we formulate this problem via a cross-layer approach with joint consideration of scheduling and routing. Although the problem formulation is in the form of mixed integer linear program (MILP), we are successful in developing a polynomial time algorithm that offers highly competitive solution. The main ideas of the algorithm include identification of key integer variables, fixing these variables via a series of relaxed linear program (LP), and tying up such integer fixing with a bottom-up tree construction. By comparing with a lower bound, we find that the proposed algorithm can provide a solution that is very close to the optimum.

In parallel to the development of CR for DSA, multiple-input multiple-output (MIMO) has widely been accepted and now implemented in commercial wireless products to increase capacity. The goal of MIMO and how it operates are largely independent and orthogonal to CR. Instead of exploiting idle channels for wireless communications, MIMO attempts to increase capacity within the same channel via space-time processing. Assuming that CR and MIMO will ultimately marry each other and offer the ultimate flexibility in DSA and spectrum efficiency, we would like to inquire the potential capacity gain in this marriage. In particular, we are interested in how such marriage will affect the capacity of a user communication session in a multi-hop CRN. We explore MIMO-empowered CR network, which we call CRN^{MIMO}, to achieve ultimate flexibility in DSA and spectrum efficiency. Given that CR and MIMO handle interference at different levels (across channels vs. within a channel), we are interested in how joint optimization of both will maximize user capacity in a multi-hop network. To answer this question, we develop a tractable mathematical model for CRN^{MIMO}, which captures the essence of channel assignment (for CR) and degree-of-freedom (DoF) allocation (for MIMO). Based on this mathematical model, we use numerical results to show how channel assignment in CRN and DoF allocation in MIMO can be jointly optimized to maximize capacity. More important, for a CRN^{MIMO} with A_{MIMO} antennas at

each node, we show that joint optimization of CR and MIMO offers more than A_{MIMO}-fold capacity increase than a CRN with only a single antenna at each node.

Acknowledgments

I would like to take this opportunity to acknowledge all the people that made a difference in my graduate study at Virginia Tech.

First and foremost, I would like to express my sincere gratitude to Prof. Y. Thomas Hou, who offered me this opportunity to come to Virginia Tech and led me into this exciting area of wireless network research. I thank his support and mentoring over the past two years. His extensive knowledge, enlightening direction, and numerous constructive suggestions made my research work positive and fruitful. I also thank him for the countless hours he has spent with me, in rewriting/editing my paper manuscripts and this thesis draft.

I would like to thank Dr. Yi Shi specially for being a constant source of inspiration, encouragement, and mentoring. I have been working with him closely since I joined Prof Hou's research group. He was always there to offer help and provided me with the right ideas to overcome the obstacles in the course of my research. I am deeply impressed by his depth of knowledge, keen research insights and patience in his guidance to my research work. I experienced and gained so much from him, both knowledge and methodology in networking research. His help is indispensable to the completion of this thesis.

I also benefited very much from Prof. Hanif D. Sherali. I highly appreciate his great help in my research work. I was fortunate to take several key courses in optimizations that are very useful for my research. In addition, he provided many constructive comments and suggestions on my drafts, which enhanced the quality of my papers significantly.

I also want to thank Prof. Yaling Yang, who serves on my thesis committee and offered valuable suggestions on my work.

I want to acknowledge my fellow students and friends at Virginia Tech, including Jia Liu, Canming Jiang, Sushant Sharma, Liguang Xie, and many others. I thank them for the discussions, cooperation, and assistance during the past two years. Their friendship has made my graduate study both fun and rewarding.

I thank my parents Min Gao and Jianzhen Jiang for everything they have offered me in my life. Without their love, support, and encouragement, I would not have finished this research work. Finally, I would like to thank my wife, Pengfei Lu. I thank her for all she has done to make my life full of joy.

Contents

List of Figures

List of Tables

Chapter 1

Introduction

1.1 Background

Since its inception, CR has quickly been accepted as the enabling radio technology for next-generation wireless communications [17, 52]. Fundamental characteristics of CR are that transmitted waveforms are defined by software and that received waveforms are demodulated by software. This is in contrast to traditional hardware-based radios in which processing is done entirely in custom-made hardware circuitry. The unique characteristics of CR promise unprecedented flexibility in radio functionalities via programmability at the lowest layer, which was once done in hardware. CR is capable of sensing available spectrum, learning and adapting, thus able to address the heart of the problem associated with spectrum scarcity (via dynamic spectrum access (DSA)) and interoperability (via channel switching). Already, CR (or its predecessor, software defined radio) has been implemented for not only cellular communications [46], but also the military [20], and public safety communications [38]. CR will also be employed as a general radio platform upon which numerous wireless applications can be implemented.

1.2 Characteristics of CR

Based on it advanced physical layer design, CR is capable of sensing available spectrum, learning, reconfiguring RF and switching to newly-selected frequency bands. These capabilities distinguish CR from other radio technologies. For a CRN, it is important to contrast it to a closely related network – multi-channel multi-radio (MC-MR) network. First, the radio technology in CR is software-based. A soft radio is capable of switching frequency bands on a per-packet basis. Further, CR can use multiple bands at the same time. In contrast, MC-MR remains hardware-based radio technology, i.e., each radio can only operate on a single channel at a time and there is no switching of channel on a per-packet basis, and the number of concurrent channels that can be used at a wireless node is limited by the number of radio interfaces. Therefore, a CR can use many more concurrent frequency bands than MC-MR. Second, in CRNs, each node may have a different set of available frequency bands (those bands not used by primary users). There may not exist a set of "common bands" for all nodes. On the other hand, a MC-MR based wireless network typically assumes that there is a set of "common bands" available for all nodes in the network. These important differences distinguish CR from MC-MR. They also bring in more flexibility as well as complexity in the algorithmic design and optimization.

1.3 New Technical Challenges

While expanding the flexibility of wireless networks, CR also brings in new technical challenges in networking research. In our problems, we aim to optimize network level performance of a multi-hop CRN. For such kind of problem, it is well understood that network performance is tightly coupled with lower layer behaviors. For example, to determine the amount of flow that can be transported between two nodes, we need to compute this link's capacity under a particular scheduling. Then we can determine how to utilize this link capacity by optimally assigning a flow rate on this link. For scheduling, before we decide if a link should be active on certain frequency bands, we should confirm that this link is indeed used in upper layer routing. For those links that are

not used for routing, we should not consider them for scheduling. Due to these inter-dependencies among layers, a cross-layer design is essential to achieve optimal CRN performance.

However, a cross-layer approach is usually highly complex and difficult, not only theoretically but also practically. Mathematically, the cross-layer design enlarges the design space. Also, such cross-layer optimization usually involves several groups of binary variables and integer variables, which make the problem extremely difficult. Moreover, the constraints and the objective function could introduce nonlinearity, which further increase the difficulty of the problem. Due to the above challenges, an analytically tractable solution with provable performance guarantee is difficult to obtain. This suggests that new ideas in algorithm design are needed.

1.4 Problems Considered in This Thesis

In this thesis, we consider the following two problems in CRNs. The first problem is on multicast communications in a CRN. In this problem, there is a set of multicast communication sessions need to be supported, each is associated with a certain flow rate. For each multicast session, there is a source node and several destination nodes. The data flow with certain rate requirement needs to be transported to each destination node. We are interested in how to support concurrent multicast sessions in a CRN such that the required network-wide resource can be minimized.

The second problem that we study in this thesis is a joint optimization of MIMO and CRN. Both CR and MIMO have the ability to exploit the spectrum efficiency. However, CR operates on the channel/band level while MIMO operates within the same channel/band. Ultimately, CR and MIMO will be combined with each other and offer the ultimate flexibility in DSA and spectrum efficiency. We would like to inquire the potential capacity gain in this combination. In particular, we are interested in how such marriage will affect the capacity of a user communication session in a multi-hop CRN. We study how to maximize the network capacity by assigning frequency bands on links and allocate antennas at each node for either data communication or interference cancellation.

1.5 Summary of Contributions

The contributions of this thesis are summarized as follows.

1.5.1 Minimum-Resource Multicast

In this work, we consider a multi-hop CRN and study how to minimize network-wide resource requirement to support a set of multicast communication sessions, each with a certain flow rate that must be transported. We follow a cross-layer approach, with joint formulation of frequency band scheduling and multicast routing. Although the problem formulation is in the form of mixed integer linear program, we successfully design a polynomial time algorithm that offers highly competitive solution. The main ideas of the algorithm include identification of key integer variables, fixing these variables via a series of relaxed linear program (LP), and tying up such integer fixing with a bottom-up tree construction. By comparing with a lower bound, we find that the proposed algorithm can provide a near-optimal solution.

1.5.2 Joint Optimization of MIMO and CRN

With CR and MIMO handling interference at channel and co-channel levels, we raise the following fundamental question: Will joint optimization of CR (via channel assignment) and MIMO (via DoF allocation) offers more than A_{MIMO}-fold capacity increase? The answer to this question is important since it also answers the question that whether or not joint optimization of both technologies is necessary, given that MIMO can already have A_{MIMO}-fold capacity increase via spatial multiplexing. In this work, we investigate this fundamental question. We develop a tractable mathematical model for multi-hop MIMO-empowered CR networks. The mathematical model captures the essence of channel assignment (for CR) and DoF allocation (for MIMO). This joint optimization problem is formulated into a mathematical program with the goal of maximizing the minimum rate among user sessions. We obtain numerical results with this mathematical model which show

how channel assignment in CRN and DoF allocation in MIMO can be jointly optimized to maximize capacity. Moreover, we give an affirmative answer that the joint optimization of CR and MIMO can offer more than A_{MIMO}-fold capacity increase for a CRN with only a single antenna at each node.

1.6 Thesis Outline

The remainder of this thesis is organized as follows. In Chapter 2, we study the multicast communications in CRNs. We formulate the minimum resource multicast for CRNs problem via a cross-layer approach by taking consideration of scheduling and routing jointly. Then we are propose a polynomial time algorithm that offers highly competitive solution. In Chapter 3, we study the joint optimization of MIMO and CRN. We develop a tractable mathematical model for CRN^{MIMO}, which captures the essence of channel assignment (for CR) and degree-of-freedom (DoF) allocation (for MIMO). Based on this mathematical model, we use numerical results to show how channel assignment in CRN and DoF allocation in MIMO can be jointly optimized to maximize capacity. Then we show that joint optimization of CR and MIMO offers more than A_{MIMO}-fold capacity increase than a CRN with only a single antenna at each node. In Chapter 4, we summarize our results in this thesis and present our future research directions.

Chapter 2

Minimum-Resource Multicast Communications

2.1 Introduction

Recently, CR has been considered as the radio platform for multi-hop ad hoc networks (see, e.g. [19, 41]). An important service that must be supported by ad hoc networks is multicast. Although there is an abundance of research on multicast in ad hoc networks (see Section 2.2), those results cannot be applied to a CR ad hoc network, due to the complexity associated with a CR node (e.g., multiple available frequency bands, difference in available bands from neighboring nodes). In addition, a single-layer approach (e.g., multicast routing [37]) is overly simplistic when resource optimization (i.e., minimizing network resource) is also an objective, in addition to multicast connectivity. In this context, a cross-layer approach is usually necessary, which should include joint consideration of multiple lower layers, in addition to network layer. However, such joint formulation is usually highly complex and difficult, as we shall soon see in this chapter (Section 2.4).

It is important to contrast a CR ad hoc network to a closely related network – MC-MR network [1, 25, 26]. First, MC-MR employs traditional hardware-based radio technology and thus each

radio can only operate on a single channel at a time and there is no switching of channel on a per-packet basis. Thus, the number of concurrent channels that can be used at a wireless node is limited by the number of radios. In contrast, the radio technology in CR is software-based; a soft radio is capable of switching frequency bands on a per-packet basis. As a result, the number of concurrent frequency bands that can be used by CR is typically much larger than that can be supported by MC-MR. Second, a common assumption for MC-MR is that there is a set of common channels available for every node in the network. Such assumption is hardly true for a CR networks (CRN), in which each node may have a different set of available frequency bands (those bands not used by primary users). An even more profound advance in CR technology is that future CR can work on non-contiguous channels for transmission/reception. These important differences between MC-MR and CR warrant that the algorithm design for a CR ad hoc network is substantially more complex than that for a MC-MR network. In some sense, a MC-MR network can be considered as a special case of a CRN. Thus, algorithms designed for a CR ad hoc network can be extended to address a MC-MR network while the converse is not true.

In this chapter, we consider a multi-hop CR ad hoc network and study how to minimize network-wide resource requirement to support a set of multicast communication sessions. In this network, the available frequency bands at each node may be different and two neighboring nodes can communicate with each other only if they share at least one common band. For each multicast session, there is a source node and a group of destination nodes. Further, there is a flow bit rate that must be transported from the source node to its group of destination nodes. To minimize required network resource (measured in network-wide bandwidth-footprint product (BFP)) to support these multicast communication sessions, we find that it is necessary to follow a cross-layer approach, with joint formulation of frequency band scheduling and multicast routing. Through mathematical modeling, we formulate the optimization problem as a mixed-integer linear programming (MILP).

In this chapter, we give the development of a polynomial-time algorithm to the cross-layer optimization problem (MILP) that offers a highly competitive solution. We observe that although there are many integer variables in the problem formulation, the binary scheduling variable (for band assignment on each link) is the core variable and its determination will help determine other

integer variables. Based on this observation, we focus on fixing these scheduling variables through an iterative process via a relaxed linear program (LP) of the original problem. Further, during each iteration, we take an explicit topological consideration during the fixing of these scheduling variables and follow a "bottom-up" approach (from leaf to root) for multicast tree construction. At the end of the last iteration, all these integer variables will be fixed and the values for the other variables can be obtained by solving a LP.

To measure the performance of our proposed solution, we compare it to a lower bound obtained via an optimization solver (CPLEX). Note that the optimal solution (unknown) is between the solution obtained by our algorithm and the lower bound by CPLEX. Simulation results show that the solution obtained by our algorithm is very close to the lower bound, thus suggesting that the solution by our algorithm is even closer to the optimum.

The remainder of this chapter is organized as follows. Section 2.2 reviews related work. In Section 2.3, we study the characteristics associated with multicast communications in a CR ad hoc network, thus laying the ground for mathematical modeling. In Section 2.4, we present mathematical model for our problem. In Section 2.5, we present the solution to our optimization problem. Section 2.6 presents simulation results and demonstrates its near-optimal performance. Section 2.7 concludes this chapter.

2.2 Related Work

In this section, we review related work on multicast in multi-hop ad hoc networks. We organize this section as follows. First, we examine prior efforts on multicast for ad hoc networks with each node equipped with single traditional radio. Then we review related work on multicast for MC-MR ad hoc networks. To the best of our best knowledge, there is so far no result for multicast problem for a multi-hop CR ad hoc network.

There has been a large body of work on multicast for ad hoc network with each node equipped with a single hardware-based (traditional) radio, e.g., [2, 6, 8, 11–13, 18, 27, 28, 34, 48–51]. Among

these works, the focus in [6, 8, 48–51], was on energy-efficient multicast routing, while the focus in [11–13, 18, 34], was on lifetime-optimal multicast, either with directional antennas or omni-directional antennas. In [2,27,28], the authors studied multicast throughput maximization problem.

In the context of MC-MR network, multicast was studied in [33,53]. In [33], the authors studied channel assignment for multicast problem in MC-MR wireless mesh networks. Here, the authors first assumed that there is a pre-built multicast tree (e.g., via multicast ad-hoc on-demand distance vector (MAODV) protocol). Then they proposed a channel assignment algorithm which greedily assigns a channel to each transmitting node so as to minimize the interference among nodes in the multicast tree. In [53], Zeng et al. studied a joint routing and channel assignment problem for MC-MR wireless mesh networks with the goal of maximizing throughput. The authors proposed a layer-by-layer decoupled heuristic algorithm called multi-channel multicast (MCM). The MCM algorithm builds a multicast tree via two steps. First, it uses a breadth-first-search (BFS)-based algorithm to obtain level information for each node; then it constructs a tree from the lowest level and follows a greedy algorithm in selecting parent nodes. Once the multicast tree is obtained, the channel assignment part commences, where authors proposed two algorithms, depending on whether the channels are orthogonal or overlapping.

2.3 Understanding Multicast Problem in a CRN

In this section, we explore some characteristics associated with the multicast problem in a CRN. Such characteristics are not only important to help us understand the underlying difficulties in this problem, but also set the stage for our mathematical modeling and problem formulation in Section 2.4.

Before we describe each characteristic in detail, let us recall the general setting for an ad hoc CRN under investigation. The network that we consider in this chapter is an ad hoc network with each node equipped with a CR. There is a set of available frequency bands for communication at each node, depending on its location. Such bands may include those bands that are currently

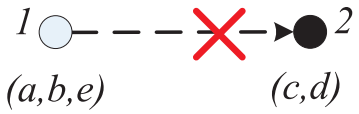

Figure 2.1: Communication between two nodes cannot take place in the absence of a common frequency band.

not in-use by primary users. Given the differences in geographical location, the set of available frequency bands at one node may be different from those at another node in the network. This is also a unique feature that distinguishes an ad hoc CRN from a conventional MC-MR network.

We organize this section as follows. From Section 2.3.1 to 2.3.5, we discuss some unique and interesting characteristics associated with the multicast problem in a CRN. Section 2.3.6 concludes our discussion with an example illustrating of the multicast problem and potential solution.

2.3.1 Transmission and Interference in a CRN

Under a traditional wireless network, nodes typically share the same pool of frequency bands. Whether two nodes can communicate with each other or not is only limited by the transmission range. But in a CRN, there is an additional constraint that must be considered. That is, we must make sure that there is at least a common band that is available between the two nodes. If no such band is available, then the two nodes will not be able to communicate with each other. Figure 2.1 illustrates this constraint with a two-node example. Here node 1 has a set of available bands $\{a, b, e\}$ while node 2 has a set of available bands $\{c, d\}$. Since there is no common band between the two sets, nodes 1 and 2 cannot communicate with each other.

Under a traditional wireless network, whether a node can interfere another node or not is only determined by the interference range. Again, such interference relationship is based on the assumption that all nodes in the network operate on the same frequency band. But for an ad hoc CRN, the interference relationship is much more complicated, due to the potential difference in the set of available frequency bands at different nodes. As an example, Fig. 2.2 shows three pairs

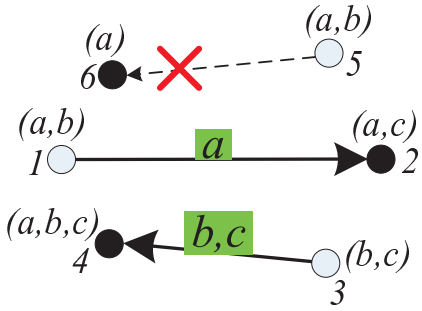

Figure 2.2: Additional bands help mitigate interferences in the network and enlarge scheduling space.

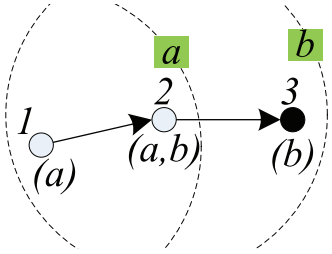

Figure 2.3: Achieving full duplex via different bands.

of nodes. Node 1 transmits to node 2 on band a while node 3 transmits to node 4 on band b and c. There is no interference on node 2 (from node 3) due to node 3's transmission is on different bands. But node 5 is not allowed to transmit to node 6 on band a due to its interference on node 2.

2.3.2 Full Duplex via Different Bands

Under a traditional wireless network, a node typically cannot transmit and receive at the same time, due to half-duplex (self-interference) constraint on the same time. But for an ad hoc CRN, full duplex is possible, if a node transmit and receive on *different* bands. An example is given in Fig. 2.3, where the available bands at nodes 1, 2, and 3 are $\{a\}$, $\{a, b\}$, and $\{b\}$, respectively. Therefore, the common band between nodes 1 and 2 is band a and that between nodes 2 and 3 is band b. In this case, node 2 can transmit to node 3 on band b while receiving from node 1 on

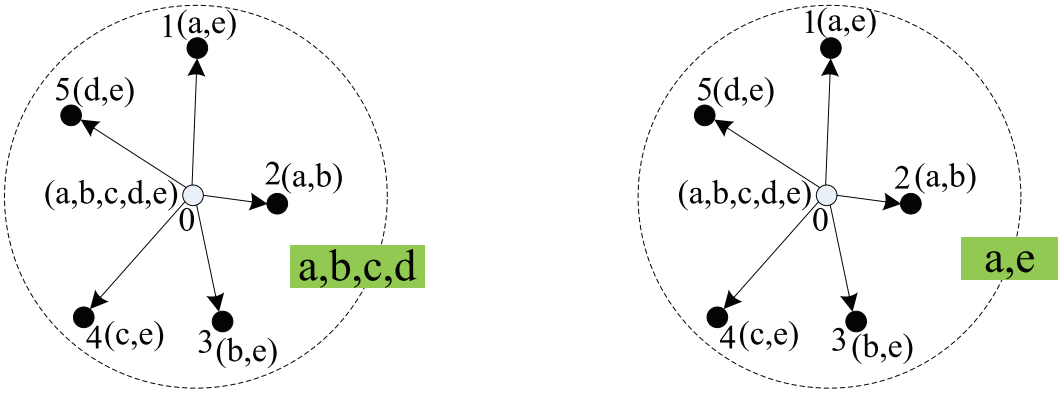

(a) Node 0 uses 4 bands $\{a, b, c, d\}$ to cover all 5 neighboring nodes.

(b) Node 0 uses 2 bands $\{a, e\}$ to cover all 5 neighboring nodes.

Figure 2.4: Design space for scheduling bands for one-hop multicast.

band a.

2.3.3 Multicast Band Scheduling

Under a traditional ad hoc wireless network, a transmission at a node can be heard by all its one-hop neighboring nodes. This is true since all nodes are assumed to operate on the same band. As discussed, this may not be true in an ad hoc CRN as the available bands on each node may be different and two nodes can communicate with each other only if they share a common band. Due to such diversity in available bands between a source node and its one-hop neighboring nodes, it might be necessary to employ multiple bands to achieve one-hop multicast. As an example, in Fig. 2.4, suppose we have a source node 0 with available bands $\{a, b, c, d, e\}$, with node 0's one-hop neighboring nodes being 1, 2, 3, 4, and 5. Suppose the available bands at these five nodes are $\{a, e\}$, $\{a, b\}$, $\{b, e\}$, $\{c, e\}$, and $\{d, e\}$, respectively. It is not difficult to verify that there does not exist one common band that node 0 can use to multicast to all five neighboring nodes. So multiple bands must be used at node 0 to achieve this purpose.

Figures 2.4(a) and (b) show two possible realizations for this objective, where in Fig. 2.4(a), node 0 uses four bands $\{a, b, c, d\}$ to cover all five nodes whereas in Fig. 2.4(b), node 0 uses only

(a) Unicast capacity.

(b) One-hop multicast capacity.

Figure 2.5: Computation of one-hop multicast capacity.

two bands $\{a, e\}$ for the same purpose. Given such difference in band usage, there exists a design (or optimization) space to decide which set of bands to use. The problem is further complicated by the fact that finding the minimum set of bands to cover one-hop neighboring node does not mean that the total network-wide usage of frequency bands will be minimized, which is our optimization objective (see Section 2.4.4). This is because a multicast tree will consist of multiple hops and there is inter-dependency in terms of band usage and interference within the same tree and among different trees.

2.3.4 One-Hop Multicast Capacity

A nice property associated with a wireless network is the so-called *wireless multicast advantage* (WMA) [51], which refers to the phenomenon that the transmission at a node will be heard by all of its one-hop neighboring nodes. But the distances between the transmitting node and its various one-hop neighboring nodes may be different. Given such difference in distances, the received signal strength at each of the one-hop neighboring nodes will be different, leading to different capacity. For multicast communication, it is necessary to have branch of the tree carry the same traffic flow rate. For a one-hop multicast, the capacity of this hop is therefore limited by the node that is farthest away from the transmitting node.

As an example, Fig. 2.5 shows that node 1 uses WMA to transmit to both nodes 2 and 3. The distances from nodes 2 and 3 to node 1 are different, with node 3 being farther away from node 1. The received signal power at node 3 is lower than that at node 2 and the capacity (using Shannon's capacity formula) on link 13 is 50 while that on link $1 \rightarrow 2$ is 60. Therefore, the traffic flow on this

(a) A single-hop multicast. (b) A multi-hop multicast.

Figure 2.6: Long hop vs. short hops.

one-hop multicast is limited by the lower link capacity, which is 50.

2.3.5 Long Hop or Short Hops

In our multicast problem, there is a flow rate requirement associated with a multicast tree. To support such flow rate at a hop, it might be necessary to deploy multiple bands. On the other hand, we could break up one hop into shorter hops to cover the same multicast group. Since our objective function is to minimize the use of bands in the network, the choice of one long hop or more short hops will depend on which one will use fewer number of bands. In other words, the number of hops is also part of the optimization space.

As an example, in Fig. 2.6(a), for single hop, we need to use k different bands at node 1 to support certain flow rate to nodes 4 and 5. But if we break up this long hop into two shorter hops, we might support the same flow rate from node 1 to nodes 4 and 5 with three bands. Here, we assume the transmission power at node 1 is the same under both Figs. 2.6(a) and 2.6(b). Therefore, if $k > 3$, then we should use the multi-hop approach in Fig. 2.6(b). On the other hand, if $k < 3$, we should use the single-hop approach in Fig. 2.6(a).

The decision of using one long hop or more short hops at any stage is further complicated in our multicast problem by the fact that the distance from a source node to its multicast destination nodes could be long (i.e., many decisions along the tree) and that there are multiple multicast trees in the network.

2.3.6 An Example

We conclude our discussion in this section with an example illustrating all the points in this section. Figure 2.7(a) shows the network topology for a 12-node ad hoc network. All units (i.e., distance, bandwidth, rate, power) are normalized appropriately. In this network, node 0 wishes to set up a multicast tree to nodes 1, 4, 6, 10, and 11. The required flow rate on this multicast tree is 62. The available frequency bands at each node is given in the figure, with each band having a bandwidth of 50. The signal from i to node j is attenuated with a gain of $g_{ij} = d_{ij}^{-n}$, where n is the path loss index and is set to 4. The transmitting power P on all nodes is $4 \cdot 10^7 \eta$, where η is the Ambient noise density. Under this transmitting power, the transmission range is set to 30 and the interference range is set to 50.

Suppose the objective function is to minimize the total number of bands required to set up the multicast tree. Then Fig. 2.7(b) shows an optimal solution, which can be found via exhaustive search or our own algorithm to be presented in Section 2.5. In this optimal solution, node 0 uses band b to transmit to nodes 3 and 7; node 3 then uses band d to forward this rate to destination nodes 1 and 4 while node 7 uses bands a and e to forward this rate to nodes $6, 10$ and 11. The total number of bands used in the optimal solution is 4 (i.e., bands b, d, a, e).

Now let's take a close look at this optimal solution. We enumerate our points as follows.

1. Although destination node 4 is within one-hop of source node 0, node 0 cannot transmit to node 4 directly because there is no common band between the two nodes, as discussed in Section 2.3.1. Therefore, a multi-hop solution from node 0 to node 4 is necessary.

2. Destination node 4 uses band d to receive the data from node 3. At the same time, node 7 is using bands a and e for transmission. But such transmission on bands a and e do not interfere node 4 since node 4 neither has nor uses these two bands (also see Section 2.3.1).

3. For nodes 3 and 7 that both transmit and receive, full duplex is achieved by using different bands at these nodes (also see Section 2.3.2).

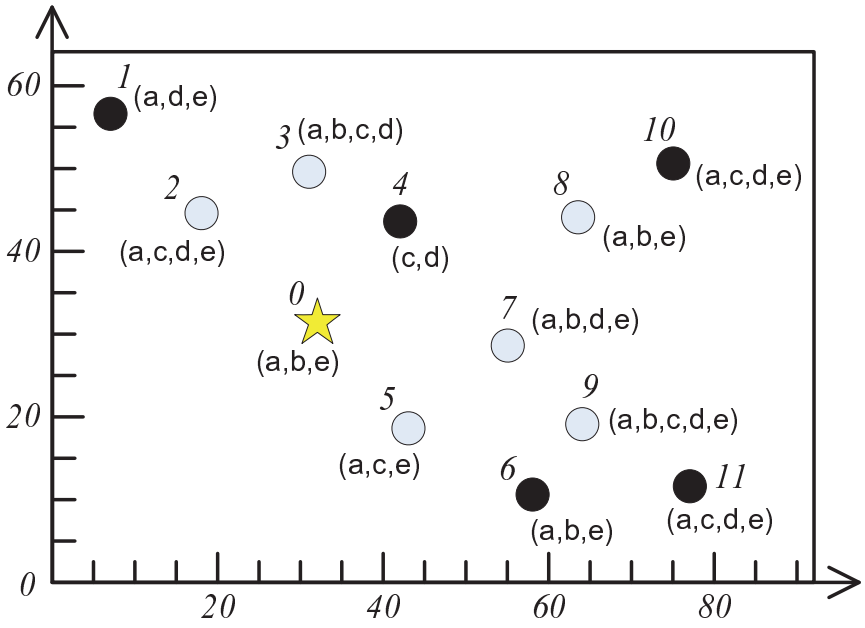

(a) A CRN example.

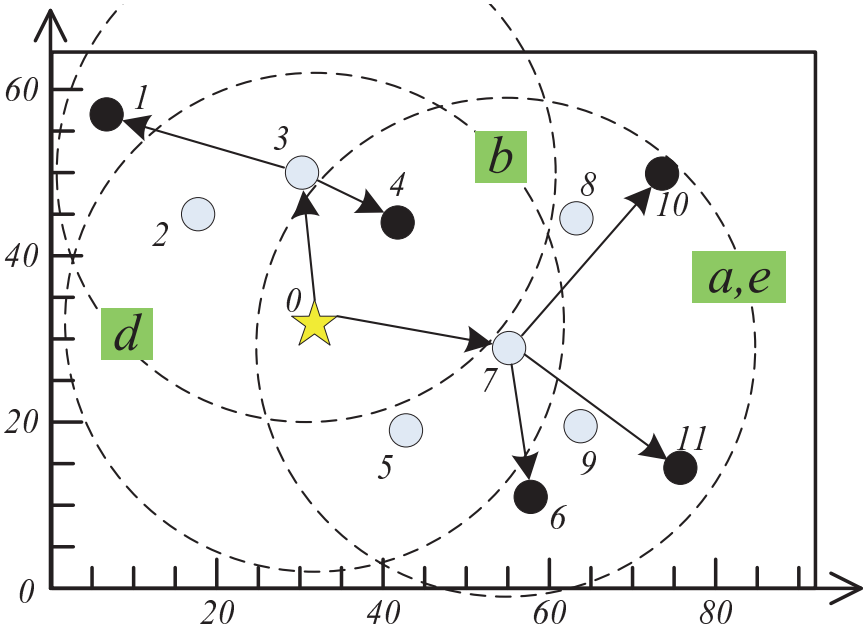

(b) Optimal solution to the CRN example.

Figure 2.7: A CRN example.

4. In this optimal solution, node 7 uses bands a and e to transport a flow rate of 62 to nodes 6, 10, and 11. It turns out that bands a and e is the minimum set of common bands among nodes 7, 6, 10, and 11, which happens to be able to support a flow rate of 62. Should flow rate requirement on the multicast group increases, the tree will change and the set of bands in each one-hop multicast will also change (also see Section 2.3.3).

5. Recall in Section 2.3.4, the capacity of one-hop multicast is limited by the node that is farthest away from the transmitting node. As show in this optimal solution, for the one-hop multicast at node 7, node 10 is the farthest node away from 7. We find the capacity from node 7 to node 10 on one band (e.g., a) is only 51.3. Therefore, a second band (i.e., e) is necessary to support a multicast flow rate of 62.

6. In this optimal solution, node 7 uses bands a and e to transport a flow rate of 62 to nodes 6, 10, and 11 in one-hop. It can be shown that node 7 may use multiple hops to nodes 10 (via 8) and 11 (via 9). But that turns out to be a sub-optimal solution. As discussed in Section 2.3.5, there is no definitive rule of whether to use one long hop or more short hops. Given that we will consider multiple multicast tree in this chapter (see Section 2.4), the choice of using one long hop or more short hops at a node is also part of the optimization problem.

In this section, we explored a number of characteristics (or difficulties) associated with multicast communication in an ad hoc CRN. In the next section, we formalize our problem with mathematical model. In particular, we study the general case where there are multiple multicast sessions (or groups) in the network.

2.4 Mathematical Modeling

We consider a CRN consisting of a set of $\mathcal{V}$ nodes. At each node $i \in \mathcal{V}$, there is a set of $\mathcal{B}_i$ available frequency bands that can be used for communications. As discussed, $\mathcal{B}_i$ may represent the set of bands that are unused by primary users and may be different at each node due to geographical

difference. Denote the set of commonly available bands between nodes i and j as $\mathcal{B}_{ij} = \mathcal{B}_i \bigcap \mathcal{B}_j$.

Denote $\mathcal{L}$ the set of multicast sessions in the network, with each multicast session consisting of a source node and multiple destination nodes. For a multicast session $l \in \mathcal{L}$, denote $s(l)$ the source node, $\mathcal{D}(l)$ the set of destination nodes, and $r(l)$ the rate requirement (in b/s). For each multicast session, we consider a tree structure for multicast routing. That is, all the nodes involved in the multicast session l form a tree rooted at node $s(l)$ and with all the nodes $\mathcal{D}(l)$ in the tree. Note that a destination node does not have to be a leaf node on the tree: it may be an intermediate node within the tree. Further, a source node and a destination node of session l may also serve as a relay node for some other session.

We organize this section as follows. Section 2.4.1 presents scheduling and interference models. Section 2.4.2 presents modeling for multicast flow routing. Section 2.4.3 shows how to compute capacity for one-hop multicast. Section 2.4.4 elaborates the objective of minimizing the total bandwidth requirement and formulates the problem. Table 2.1 lists all the notation used in this chapter.

2.4.1 Interference Modeling and Scheduling

Scheduling for transmission at each node in the network can be done either in frequency domain or time domain. In this chapter, we consider scheduling in frequency domain in the form of assigning frequency bands (channels). Since time domain based formulation is similar to that for frequency domain, it can be shown that our approach can be extended to time domain based formulation as well. We first define the following binary variable for frequency band scheduling,

$$u_{ij}^m(l) = \begin{cases} 1 & \text{if band } m \text{ is used on link } i \to j \text{ for session } l, \\ 0 & \text{otherwise,} \end{cases}$$

where $l \in \mathcal{L}, i \in \mathcal{V}, m \in \mathcal{B}_{ij}, j \in \mathcal{T}_i^m, j \neq s(l)$, and $\mathcal{T}_i^m$ is the set of nodes to which node i can transmit on band m. As we have discussed in Section 2.3.1, this set includes nodes that are within the transmission range of node i and have the same available band m, i.e., $\mathcal{T}_i^m = \{j : j \in \mathcal{V}, 0 <$

Table 2.1: Notation in Chapter 2

Symbol	Definition
$\mathcal{B}_i$	The set of available bands at a node $i \in \mathcal{V}$
$\mathcal{B}$	The union of available bands among all the nodes in the network, $\mathcal{B} = \bigcup_{i \in \mathcal{V}} \mathcal{B}_i$
$\mathcal{B}_{ij}$	The set of available bands on link $i \rightarrow j$, $\mathcal{B}_{ij} = \mathcal{B}_i \bigcap \mathcal{B}_j$
c_{ij}^m	The unicast capacity from i to j on band m
c_i^m	The one-hop multicast capacity at node i on band m
$\mathcal{D}(l)$	The set of destination nodes of a session $l \in \mathcal{L}$
d_{ij}	Distance between nodes i and j
$e_{ij}(l)$	Binary indicator to mark whether or not link $i \rightarrow j$ is used for session l
$f_{ij}^m(l)$	$f_{ij}^m(l) = u_{ij}^m(l) \cdot c_i^m$
g_{ij}	Path attenuation loss from node i to node j
$\mathcal{I}_j^m$	The set of nodes that can make interference at node j on band m
$\mathcal{L}$	The set of multicast sessions in the network
n	Path loss index
P	The transmission power at a transmitter
R_T, R_I	The transmission and interference ranges
$r(l)$	Multicast flow rate of session l
$s(l)$	Source node of multicast session l
$\mathcal{T}_i^m$	The set of nodes that node i can transmit to and receiving from on band m
$\mathcal{T}_i$	The set of nodes that node i can communicate with on at least one of its bands, $\mathcal{T}_i = \bigcup_{m \in \mathcal{B}_i} \mathcal{T}_i^m$
$u_{ij}^m(l)$	Binary indicator to mark whether or not band m is assigned to link $i \rightarrow j$ for session l
$\mathcal{V}$	The set of nodes in the network
W	Bandwidth of a frequency band
$x_i^m(l)$	Binary indicator to mark whether or not band m is used for transmission at node i for session l
$y_j(l)$	The depth of node j in the multicast tree for session l
η	Ambient Gaussian noise density

$d_{ij} \leq R_T, m \in \mathcal{B}_j\}$.

Assuming the granularity of frequency bands can be made small enough for scheduling, we will assign an available band at each transmitting node to at most one multicast session $l \in \mathcal{L}$. That is, if $u_{ij}^m(l) = 1$ then $u_{iq}^m(k) = 0$ for another session k. This scheduling relationship can be written more compactly as follows.

$$u_{iq}^m(k) \leq 1 - u_{ij}^m(l) \quad (i \in \mathcal{V}, m \in \mathcal{B}_i, j \in \mathcal{T}_i^m, l \in \mathcal{L}, q \in \mathcal{T}_i^m, k \in \mathcal{L}, k \neq l) \ . \tag{2.1}$$

As we have discussed in Section 2.3.1, when node j is receiving from node i on band m, the set of nodes that can make interference to node j should keep silent on band m. This set $\mathcal{I}_j^m$ includes nodes that are within the interference range of node j and have the same available band m, i.e., $\mathcal{I}_j^m = \{p : p \in \mathcal{V}, d_{pj} \leq R_I, m \in \mathcal{B}_p\}$. Then the scheduling relationship discussed in Section 2.3.1 means $u_{ij}^m(l) = 1$ will lead to $u_{pq}^m(k) = 0$ for another link $p \rightarrow q$. This scheduling relationship can be written more compactly as follows.

$$u_{pq}^m(k) \leq 1 - u_{ij}^m(l) \ , \tag{2.2}$$

where $l \in \mathcal{L}, i \in \mathcal{V}, m \in \mathcal{B}_{ij}, j \in \mathcal{T}_i^m, j \neq s(l), k \in \mathcal{L}, p \in \mathcal{I}_j^m, p \neq i, q \in \mathcal{T}_p^m, q \neq s(k)$. Note that the so-called "self-interference" constraint, i.e., a node cannot transmit and receive on the same band, is embedded in the above constraint (by setting $p = j$). Furthermore, by setting $q = j$, the constraint prohibits the same receiving node from simultaneously receiving from two different nodes on the same band (collision), which is consistent with our scheduling in the frequency domain.

2.4.2 Multicast Routing

Multicast Tree Construction

For a multicast session $l \in \mathcal{L}$, its source node $s(l)$ must send its data with a rate $r(l)$ to a set of destination nodes $\mathcal{D}(l)$. Note that a destination node does not have to be a leaf node – it can be an internal node in the tree and helps out relaying traffic to other destination nodes.

We start our mathematical modeling with the following definition.

$$e_{ij}(l) = \begin{cases} 1 & \text{if link } i \to j \text{ is an directed edge in the multicast tree for session } l, \\ 0 & \text{otherwise,} \end{cases}$$

where $l \in \mathcal{L}, i \in \mathcal{V}, j \in \mathcal{T}_i, j \neq s(l)$, and $\mathcal{T}_i$ denotes the nodes that node i can communicate with on at least one of its bands, i.e., $\mathcal{T}_i = \bigcup_{m \in \mathcal{B}_i} \mathcal{T}_i^m$. Note that if $i \in \mathcal{D}(l)$ (i.e., a destination node) and is not on the leaf of the tree, then this destination node is an internal node of the tree and helps relay traffic to other destination nodes.

We first show the relationship between $e_{ij}(l)$ and $u_{ij}^m(l)$. If $e_{ij}(l) = 0$, i.e., link $i \to j$ is not used by the multicast tree for session l, then no band should be assigned to link $i \to j$ for session l, i.e., $u_{ij}^m(l) = 0$ for all $m \in \mathcal{B}_{ij}$. If $e_{ij}(l) = 1$, then there must be at least one band assigned to link $i \to j$ for session l. Mathematically, the above relationships can be written as follows.

$$u_{ij}^m(l) \leq e_{ij}(l) \leq \sum_{\rho \in \mathcal{B}_{ij}} u_{ij}^\rho(l) \quad (l \in \mathcal{L}, i \in \mathcal{V}, j \in \mathcal{T}_i, j \neq s(l), m \in \mathcal{B}_{ij}) \; . \tag{2.3}$$

For session l's multicast tree, the following constraints must be satisfied.

- For a node $i \in \mathcal{V}$, if it is the source node of session l, i.e., $i = s(l)$, then it must have at least one out-going edge on the tree. That is,

$$\sum_{j \in \mathcal{T}_i} e_{ij}(l) \geq 1 \quad (l \in \mathcal{L}, i = s(l)) \; . \tag{2.4}$$

- For a node $j \in \mathcal{V}$, if it is a destination node of session l, i.e., $j \in \mathcal{D}(l)$, then it must have one incoming edge. [1] That is,

$$\sum_{i \in \mathcal{T}_j} e_{ij}(l) = 1 \quad (l \in \mathcal{L}, j \in \mathcal{D}(l)) \; . \tag{2.5}$$

- For a node j that is neither the source node of session l nor one of its destination nodes, i.e., $j \neq s(l)$ and $j \notin \mathcal{D}(l)$, then it may (or may not) serve as a relay node in the tree. For either

[1] Note that flow splitting at intermediate relay nodes is not considered in this chapter.

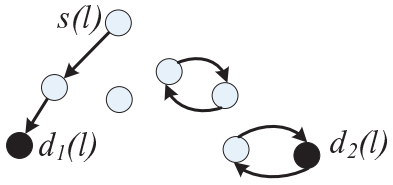

Figure 2.8: An example of potential cycle in multicast tree construction.

case, we have,

$$\sum_{i \in \mathcal{T}_j} e_{ij}(l) \leq 1 \quad (l \in \mathcal{L}, j \in \mathcal{V}, j \neq s(l), j \notin \mathcal{D}(l)) \; . \tag{2.6}$$

That is, if node j is a relay node, then there is one edge entering node j, otherwise there is no edge entering node j. Further, if there is an incoming edge to node j, then it must have at least one outgoing edge, i.e., if $\sum_{i \in \mathcal{T}_j} e_{ij}(l) = 1$, then $\sum_{q \in \mathcal{T}_j, q \neq s(l)} e_{jq}(l) \geq 1$. Otherwise, no outgoing edge should come out of node j, i.e., $\sum_{q \in \mathcal{T}_j, q \neq s(l)} e_{jq}(l) = 0$. These two scenarios can be mathematically formulated as follows.

$$\sum_{i \in \mathcal{T}_j} e_{ij}(l) \leq \sum_{q \in \mathcal{T}_j, q \neq s(l)} e_{jq}(l) \leq (|\mathcal{T}_j| - 1) \cdot \sum_{i \in \mathcal{T}_j} e_{ij}(l) \tag{2.7}$$

where $l \in \mathcal{L}, j \in \mathcal{V}, j \neq s(l), j \notin \mathcal{D}(l)$, and $(|\mathcal{T}_j| - 1)$ is an upper bound on the nodes that j can transmit to.

Cycle Prevention

It is important to realize that the constraints described for multicast tree construction cannot ensure the potential existence of cycle(s). As an example, in Fig. 2.8, source node $s(l)$, attempts to send data to two destinations nodes $d_1(l)$ and $d_2(l)$. But it is not hard to see that the incorrect solution shown in the figure satisfies all constraints for multicast tree construction. The main reason for this problem is because when a destination node (or a relay node) receives traffic and forwards to the next hop, there is no mechanism for this node to ensure that the traffic it receives is indeed from a node that is one level higher on the multicast tree (i.e., one-hop closer to the source node).

To address this problem, we define a new variable $y_j(l)$ for each node j to indicate its depth on a multicast tree for session l. Specifically, $y_j(l)$ is defined as follows.

$$y_j(l) = \begin{cases} -1 & \text{node } j \text{ is not in the multicast tree for session } l, \\ 0 & \text{node } j \text{ is the source node of multicast tree for session } l, \\ h & \text{node } j \text{ has a depth of } h \text{ in the multicast tree for session } l. \end{cases} \qquad (l \in \mathcal{L}, j \in \mathcal{V})$$

For a node j, if it is the source node, then we have

$$y_j(l) = 0 \quad (l \in \mathcal{L}, j = s(l)) \ . \tag{2.8}$$

Otherwise, when it is not in the tree, i.e., $\sum_{i \in \mathcal{T}_j} e_{ij}(l) = 0$, we have $y_j(l) = -1$; when it is in the tree, i.e., $\sum_{i \in \mathcal{T}_j} e_{ij}(l) = 1$, we have $1 \leq y_j(l) \leq |\mathcal{V}| - 1$. The above two cases can be put into the following compact form.

$$2 \sum_{i \in \mathcal{T}_j} e_{ij}(l) \leq y_j(l) + 1 \leq |\mathcal{V}| \sum_{i \in \mathcal{T}_j} e_{ij}(l) \quad (l \in \mathcal{L}, j \in \mathcal{V}, j \neq s(l)) \ . \tag{2.9}$$

Now we consider the relative depth between two nodes i and j. For the case that node i is the parent of node j, i.e., $e_{ij}(l) = 1$, then $y_j(l) - y_i(l) = 1$. For the case that node i is not the parent of node j, i.e., $e_{ij}(l) = 0$, then we have $-|\mathcal{V}| \leq y_j(l) - y_i(l) \leq |\mathcal{V}|$ (due to the fact that both $y_j(l)$ and $y_i(l)$ are within the interval $[-1, |\mathcal{V}| - 1]$). The above two cases can be stated mathematically as follows.

$$y_j(l) - y_i(l) \geq e_{ij}(l) \cdot (|\mathcal{V}| + 1) - |\mathcal{V}| \quad (l \in \mathcal{L}, j \in \mathcal{V}, j \neq s(l), i \in \mathcal{T}_j) \ , \tag{2.10}$$

$$y_j(l) - y_i(l) \leq |\mathcal{V}| - (|\mathcal{V}| - 1) \cdot e_{ij}(l) \quad (l \in \mathcal{L}, j \in \mathcal{V}, j \neq s(l), i \in \mathcal{T}_j) \ . \tag{2.11}$$

We have the following lemma.

Lemma 1. *The use of $y_j(l)$ variables ($j \in \mathcal{V}$, $l \in \mathcal{L}$) guarantees cycle free in the multicast tree for each session l.*

Proof. The proof is based on contradiction. Suppose that (2.8) to (2.11) hold and that there is a cycle for session l. Assume this cycle consists of z links $i_1 \rightarrow i_2, i_2 \rightarrow i_3, \cdots, i_{z-1} \rightarrow i_z$ and $i_z \rightarrow$

i_1, with $z \geq 2$. Then based on (2.10) and (2.11), we have $y_{i_2}(l) - y_{i_1}(l) = 1$, $y_{i_3}(l) - y_{i_2}(l) = 1$, $\cdots$, $y_{i_z}(l) - y_{i_{z-1}}(l) = 1$, $y_{i_1}(l) - y_{i_z}(l) = 1$ ($z \geq 0$). Summing up all these z equations, the left-hand-sides will all be canceled out, and the right-hand-sides add up to z, leading to $0 = z$, a contradiction to the assumption that the number of links in the cycle $z \geq 2$. This completes the proof. □

2.4.3 One-Hop Multicast Capacity and Flow Rate Constraints

The formulation for multicast tree construction in the last section only address our problem from a graph perspective. In this section, we impose constraints on capacity and flow rate on the multicast tree.

One-Hop Multicast Capacity. Now we consider a one-hop multicast where node i transmits to some of its one-hop neighbors on band m simultaneously by taking advantage of wireless multicast advantage (WMA) [51]. Denote c_i^m the capacity of this one-hop multicast. As discussed in Section 2.3.4, this capacity is limited by the node that is farthest away from node i (see Fig. 2.5), i.e., c_i^m is upper bounded by $c_{ij}^m = W \log_2(1 + \frac{g_{ij}P}{\eta W})$ for each node j that is receiving on band m, where c_{ij}^m is the unicast capacity, W is the bandwidth of band m, g_{ij} is the path attenuation loss from node i to node j, P is the transmission power, and η is the ambient Gaussian noise density. Then for each $i \in \mathcal{V}$ and $m \in \mathcal{B}_i$,

$$c_i^m \leq c_{ij}^m(l) \cdot u_{ij}^m + C \cdot [1 - u_{ij}^m(l)] \quad (\text{for all } j \in \mathcal{T}_i^m, l \in \mathcal{L}) \ , \tag{2.12}$$

where C is a sufficiently large number and means that c_i^m will not be constrained if $u_{ij}^m(l) = 0$.

In the case that node i is not using band m (i.e., $u_{ij}^m(l) = 0$ for all $j \in \mathcal{T}_i^m, l \in \mathcal{L}$), then $c_i^m = 0$. This constraint can be written as

$$c_i^m \leq C \cdot \sum_{l \in \mathcal{L}} \sum_{j \in \mathcal{T}_i^m} u_{ij}^m(l) \quad (i \in \mathcal{V}, m \in \mathcal{B}_i) \ . \tag{2.13}$$

Flow Rate Constraints. Given our modeling for one-hop multicast capacity, we now show how they serve as constraints on traffic flows. On each link, we must ensure that the flow rate on this

link does not exceed the link's capacity. We have

$$r(l) \cdot e_{ij}(l) \;\; \leq \;\; \sum_{m \in \mathcal{B}_{ij}} u_{ij}^m(l) \cdot c_i^m \quad (l \in \mathcal{L}, i \in \mathcal{V}, j \in \mathcal{T}_i) \; . \tag{2.14}$$

where $r(l)$ is the constant rate requirement for multicast session $l \in \mathcal{L}$. Note that it is possible that session l may use multiple bands on link $i \rightarrow j$, which is considered in (2.14).

To remove the nonlinear term on the right-hand-side of (2.14), we introduce a new variable $f_{ij}^m(l)$ and define it as

$$f_{ij}^m(l) = u_{ij}^m(l) \cdot c_i^m \; . \tag{2.15}$$

Then (2.14) can be rewritten as

$$r(l) \cdot e_{ij}(l) \;\; \leq \;\; \sum_{m \in \mathcal{B}_{ij}} f_{ij}^m(l) \quad (l \in \mathcal{L}, i \in \mathcal{V}, j \in \mathcal{T}_i) \; . \tag{2.16}$$

By replacing $u_{ij}^m(l) \cdot c_i^m$ with $f_{ij}^m(l)$, we need to add additional constraints for $f_{ij}^m(l)$ as follows. For integer variable $u_{ij}^m(l)$, we have the following relaxed constraints: $u_{ij}^m(l) \geq 0$, $1 - u_{ij}^m(l) \geq 0$. For variable c_i^m, we have: $c_i^m \geq 0$, $C - c_i^m \geq 0$. Multiplying each constraint involving $u_{ij}^m(l)$ by one of the two constraints involving c_i^m, and replacing the product term $u_{ij}^m(l) \cdot c_i^m$ with the new variable $f_{ij}^m(l)$, we obtain the following four constraints

$$f_{ij}^m(l) \geq 0 \quad (l \in \mathcal{L}, i \in \mathcal{V}, j \in \mathcal{T}_i, m \in \mathcal{B}_{ij}) \; , \tag{2.17}$$

$$f_{ij}^m(l) \leq c_i^m \quad (l \in \mathcal{L}, i \in \mathcal{V}, j \in \mathcal{T}_i, m \in \mathcal{B}_{ij}) \; , \tag{2.18}$$

$$f_{ij}^m(l) \leq u_{ij}^m(l) \cdot C \quad (l \in \mathcal{L}, i \in \mathcal{V}, j \in \mathcal{T}_i, m \in \mathcal{B}_{ij}) \; , \tag{2.19}$$

$$f_{ij}^m(l) \geq u_{ij}^m(l) \cdot C - C + c_i^m \quad (l \in \mathcal{L}, i \in \mathcal{V}, j \in \mathcal{T}_i, m \in \mathcal{B}_{ij}) \; . \tag{2.20}$$

Note that due to the relaxation of integer variable $u_{ij}^m(l)$ and the product operations, the above four constraints for $f_{ij}^m(l)$ are likely to be looser than that for (2.15). However, in the special case when $u_{ij}^m(l)$ is a binary variable, it can be easily verified that (2.15) is equivalent to the four constraints in (2.17) to (2.20). Therefore, it is sufficient to have five linear constraints (2.16) to (2.20) to represent (2.14).

2.4.4 Problem Formulation

Our objective is to minimize the required network-wide resource to support a set of multicast sessions $\mathcal{L}$ in the network. Resource can be measured in a number of ways. Here, we adopt a new metric called *Bandwidth Footprint Product* (BFP) to measure the spectral and spatial occupancy of multi-band radio communication. BFP was first introduced by Liu and Wang (under the name of *space-bandwidth product*) in [29] and has since successfully been used (see, e.g, [19, 41]) to measure network-wide resource usage in a CR network. Given that we assume the transmission power on each band at each node is P, the footprint by each active band is thus identical. Therefore, minimizing network-wide BFP is equivalent to minimizing network-wide bandwidth usage.

To calculate network-wide bandwidth usage, it is necessary to know which set of bands at each node has been used for transmission. For this purpose, we introduce a binary variable x_i^m, which is defined as follows.

$$x_i^m = \begin{cases} 0 & \text{band } m \text{ is not used at node } i \text{ for transmission,} \\ 1 & \text{band } m \text{ is used at node } i \text{ for transmission.} \end{cases} \qquad (i \in \mathcal{V}, m \in \mathcal{B}_i)$$

Then the objective function is to minimize $\sum_{i\in\mathcal{V}} \sum_{m\in\mathcal{B}_i} x_i^m W$. Since we assume that W is the same for each band, we can drop it from the objective function, i.e.,

$$\min \quad \sum_{i\in\mathcal{V}} \sum_{m\in\mathcal{B}_i} x_i^m \ . \tag{2.21}$$

Now we give constraints on the new variable x_i^m in the objective function. At node $i \in \mathcal{V}$ on band $m \in \mathcal{B}_i$, if $u_{ij}^m(l) = 1$ for any $j \in \mathcal{T}_i^m$ and $l \in \mathcal{L}$, then $x_i^m = 1$, i.e.,

$$u_{ij}^m(l) \le x_i^m \quad (\text{for all } j \in \mathcal{T}_i^m \text{ and } l \in \mathcal{L}) \ . \tag{2.22}$$

Otherwise, at node $i \in \mathcal{V}$ on band $m \in \mathcal{B}_i$, if $u_{ij}^m(l) = 0$ for all $j \in \mathcal{T}_i^m$ and $l \in \mathcal{L}$, then $x_i^m = 0$, i.e.,

$$x_i^m \le \sum_{l\in\mathcal{L}} \sum_{j\in\mathcal{T}_i^m} u_{ij}^m(l) \ . \tag{2.23}$$

In summary, our optimization problem is to minimize network-wide BFP, i.e., (2.21), subject to the constraints in (2.1)–(2.13), (2.16), (2.18) – (2.20), (2.22), and (2.23). In the formulation, $W, |\mathcal{V}|, |\mathcal{T}_j|, \eta, g_{ij}, c_{ij}^m, C, P$, and $r(l)$ are constants, while $c_i^m \geq 0$, $f_{ij}^m(l) \geq 0$ are continuous variables, $y_j(l)$ is an integer variable within interval $[-1, |\mathcal{V}| - 1]$, and $u_{ij}^m(l)$, $e_{ij}(l)$, and x_i^m are binary variables. This is a mixed integer linear program (MILP), which is NP-hard in general [10]. Although an optimization solver (e.g., CPLEX) can obtain a solution for small-sized networks via branch-and-cut procedure [31] (exponential complexity), the time required for medium- or large-sized networks is prohibitively high.

2.5 A Proposed Solution

In this section, we propose a polynomial-time solution to our optimization problem that offers very competitive performance. The main mathematical approach employed by the solution is to fix a set of integer variables iteratively via a relaxed LP of the original problem. During each iteration, we take explicit topological consideration when fixing integers and follow a "bottom-up" approach (from leaf to root) for tree construction. In the rest of this section, we give details of these two key ideas in our solution.

2.5.1 Sequential Fixing of u-Variables

Main Idea. For the original MILP problem, we observe that u variables have special significance. By definition, $u_{ij}^m(l)$ is a binary indicator to mark whether or not band m is assigned to link $i \rightarrow j$ for session l. In other words, $u_{ij}^m(l)$'s are scheduling variables. We find that once the values for $u_{ij}^m(l)$'s are all determined, the values for e, y and x variables can be determined by (2.3), (2.8) – (2.11), and (2.22) – (2.23), respectively. Subsequently, the original MILP problem can be reduced to a LP, which can be solved in polynomial time. Thus, the key step in solving the MILP problem is the determination of these binary u variables.

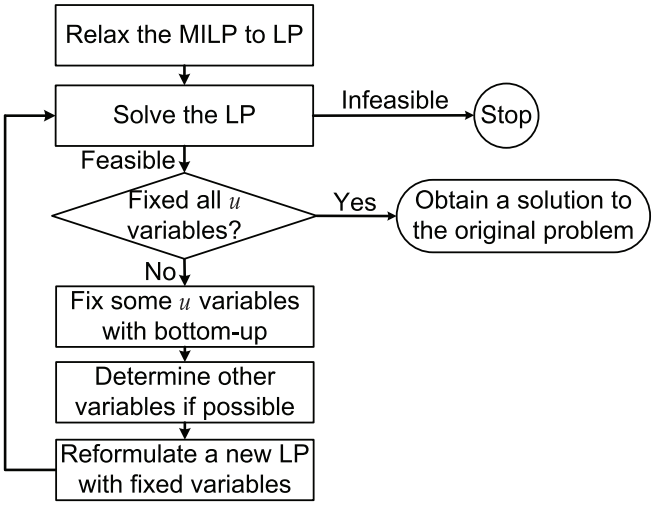

Figure 2.9: Flow chart of proposed solution.

In our proposed solution, we will consider a special subset of the $u_{ij}^m(l)$ variables at each iteration and fix some of them during the iteration. The choice of such subset of $u_{ij}^m(l)$'s will be explained in detail in Section 2.5.2. Here, we will first give a basic idea on how the algorithm works.

At each iteration, we will solve a LP problem containing those $u_{ij}^m(l)$'s (that are yet to be determined) being relaxed from their strict integer constraints, i.e., can take continuous values. Depending on the value of these $u_{ij}^m(l)$'s in the LP solution, we will consider a special subset of $u_{ij}^m(l)$'s and assign 1 to one (or more of them) permanently. Note that the fixing of some u variables at each iteration will also lead to the fixing of relevant x, e, and y variables as well as other closely related u variables through those constraints that relate them. As the iteration continues, more and more $u_{ij}^m(l)$'s will be "fixed" to binary values (1 or 0) permanently and eventually all of them will be fixed. At the end of the last iteration, all these integer variables will be fixed and the values for the other variables can be obtained by solving a LP.

Some Details. The flow chart of the proposed solution is shown in Fig. 2.9. Before the first iteration, we relax all the binary variables. That is, we relax all binary integer variables u, x and e to interval $[0, 1]$ and relax integer variables y to interval $[-1, |\mathcal{V}| - 1]$. The relaxation of all these

integer variables in the original MILP problem leads to a LP problem.

After solving this LP, if it is infeasible, then the algorithm stops, i.e., we do not have a feasible solution to support the set of $\mathcal{L}$ multicast sessions in the network. Otherwise, we have a feasible solution to the LP with each $u_{ij}^m(l)$ having a value within the interval $[0, 1]$. In the first iteration, since none of the u variables have been fixed yet, we will consider a special subset of u variables (see Section 2.5.2) and fix one or more of the u variables to 1 based on their closeness to 1.

Note that the fixing of some u variable to 1 is likely to lead to additional fixing of x, e, y, as well as other u variables in the same iteration. To see this, let's suppose $u_{ij}^m(l)$ has just been fixed to 1 in this iteration. Then it is not hard to see that we can further fix more variables' values. That is, by (2.22), we can fix x_i^m to 1; by (2.1), we can fix corresponding $u_{iq}^m(k)$ to 0; by (2.2), we can fix corresponding $u_{pq}^m(k)$ to 0 for all p and k , then we can further set x_p^m to 0 by (2.13); by (2.3), we can also fix $e_{ij}(l)$ to 1. Once $e_{ij}(l)$ has been set to 1, then by (2.5) and (2.6), we can further set corresponding $e_{pj}(l)$ to 0. After $e_{pj}(l)$ is set to 0, then by (2.3), we can set $u_{pj}^m(l)$ to 0 for all m.

With all those fixed variables in this and past iterations, we can build a new LP and move on to the next iteration. Eventually, all the u variables will be fixed, along with integer variables x, e, and y and a feasible solution to our problem may be obtained.

2.5.2 Bottom-Up Fixing of Selected u Variables

We now give details on what special subset of u variables that we will consider for fixing in each iteration. Recall that our goal is to obtain a multicast tree for each session once all u variables are fixed. If we fix u variables solely based on its closeness to 1 at each iteration (without any joint topological consideration), then we find that the tree construction process is rather chaotic and has the tendency to yield no solution for a session. As a result, we conclude that it is most important to incorporate topology consideration (i.e., tree construction) into the fixing of u variables.

There are two possible approaches to include tree construction consideration in fixing u variables. A natural approach is to construct a tree for a session following a "top-down" approach,

(a) Node j is a destination node of a multicast session l.

(b) Node j already has a route (fixed in previous iterations) to a destination node of session l.

Figure 2.10: Selection of subset of u variables to be fixed at each iteration.

i.e., from the root (source node) toward its leaf nodes (destination nodes). The problem with a top-down approach is that when we consider a set of u variables at a node, it is difficult to determine how each candidate u variable that is eligible for fixing is related to each destination node. That is, a top-down approach of fixing u variables at a node lacks directional information to the destination nodes. As a result, such approach suffers from directional "blindness" in fixing u variables and is thus not chosen in our approach.

On the other hand, if we start considering those candidate u variables that are eligible for fixing at the destination nodes and working toward the source node (i.e., "bottom-up" approach), then the direction-blindness problem associated with top-down approach can be avoided. For this reason, we adopt bottom-up fixing in our solution. Specifically, when we fix u variables, we only consider a subset of those $u_{ij}^m(l)$'s with either node j being a destination node of a multicast session l, or node j having at least one route (which has already been fixed in previous iterations) to a destination node of session l (see Fig. 2.10). Among all those eligible u variables, we choose the one that is the largest (closest to 1) and fix it to 1. That is, the fixing of u variables is specifically tailored to the bottom-up construction of a multicast tree for the session. We call this *topology-driven* fixing algorithm.

Another mechanism that we employ in bottom-up tree construction is *subtree merging.* That is, we attempt to exploit WMA as much as possible by joining multiple subtrees with the same node one hop closer to the root. This idea is best illustrated in Fig. 2.11 where two subtrees with

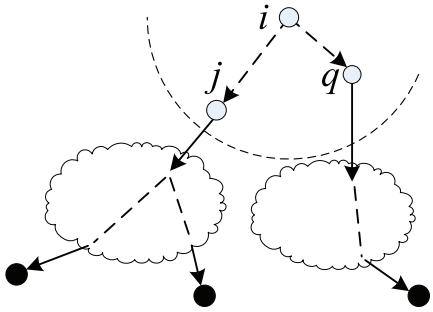

Figure 2.11: Merge of two subtrees in bottom up fixing due to a local broadcast.

current root nodes j and q are combined together at node i (one hop closer to the source node) with one local broadcast (WMA). However, such joining of multiple sub-trees during multicast construction is performed only when certain criteria are met. In particular, after $u_{ij}^m(l)$ is fixed to 1 (i.e., the transmission from node i to node j is performed by a local broadcast), we will use the same local broadcast at node i to cover another subtree with root at q (i.e., fix $u_{iq}^m(l)$ to 1) if (i) $u_{iq}^m(l) > 0$ in the current relaxed LP solution;[2] and (ii) adding node q into this one-hop multicast group does not increase the total number of required bands at node i.

2.5.3 Post-Sweep Procedure

After we build the multicast trees and assign bands to each links by the above bottom-up fixing steps (i.e., we obtain a solution to the original MILP problem), it is possible that we can further improve the solution by a post-sweep procedure which can eliminate unnecessary transmissions.

Before describing the procedure, we show an example. Fig. 2.12(a) shows a part of the tree for multicast session l, where node i is transmitting to nodes j_1, j_2, j_3 on bands m_1, m_2, and node p is transmitting to node j_4 on band m_3. In this example, when node p transmits on band m_3, nodes j_1 and j_2 can also receive the data and band m_3 is enough for the transmission from node p to

[2]Otherwise (i.e., $u_{iq}^m(l) = 0$ in the relaxed LP solution), assigning $u_{iq}^m(l)$ to 1 is likely to lead to poor or infeasible solution as doing so is not recommended by the current LP solution.

(a) Node i is transmitting to nodes j_1, j_2, j_3 on band m_1, m_2.

(b) Nodes j_1, j_2 been detached from node i and attached to node p, the transmission on band m_2 at node i can be removed.

Figure 2.12: Example for post-sweep procedure.

Proposed Algorithm

1. Set up initial relaxed LP problem.
2. Solve the relaxed LP problem. If it is infeasible, then stop and we cannot find a solution to the original problem.
3. If all u variables are fixed, then we have an solution to the original problem, goto step 8. Otherwise, goto next step.
4. Select $u_{ij}^{m}(l)$ that has the largest value among all unfixed u variables with j is either a destination node in $\mathcal{D}(l)$ or has a route to a destination node in $\mathcal{D}(l)$.
5. Find any other node that can be covered by this transmission. The corresponding u variables are also selected to be fixed as 1.
6. Based on constraints (2.1)–(2.7), (2.9)–(2.11), (2.22), and (2.23), fix more u, e, x, and y variables.
7. Reformulate a LP problem with newly fixed variables and goto step 2.
8. Perform the post-sweep procedure to refine the solution.

Figure 2.13: Pseudocode of proposed algorithm.

nodes j_1 and j_2. Then if we detach nodes j_1 and j_2 from transmitting node i and attach them to node p, the transmission on band m_1 or m_2 at node i can be eliminated since one band is enough to support the transmission from node i to node j_3, as shown in Fig. 2.12(b).

To summarize, the post-sweep procedure runs by several iterations. Within each iteration, there is an outer loop which goes over each transmitting node p by breadth first search (BFS), and an inner loop which goes over each transmitting node i by BFS. For those $i \neq p$, we consider the subset of children nodes of i that satisfy (i) they are within the transmission range of node p; (ii) they can receive the data from node p on some bands and will not be interfered by other transmission on these bands; (iii) these bands provide enough capacity for the bit rate requirement. If we detach such subset of children from node i and attach them to node p will reduce the bandwidth usage at node i, then we modify the tree accordingly. Furthermore, after this switching of parent nodes, if any node becomes a leaf node but it is not a destination node, we should remove the transmission coming from its parent. For example, in Fig. 2.12(a), if j_3 is not in the tree, then after switching the parent of j_1, j_2 to node p, we should not only eliminate the transmission on bands m_1, m_2 at node i, but also remove the transmission from s to node i if i is not a destination node. We continue running this sweep iteration until no further improvement can be achieved.

Since the total number of transmissions in the first solution is bounded by $O(|\mathcal{N}| \cdot |\mathcal{B}| \cdot |\mathcal{L}|)$, and each iteration has improvement thus will reduce the number of transmissions, the total number of the iteration is polynomial. Within each iteration, the algorithm performs polynomial operations, therefore the post-sweep procedure is also polynomial. And the complexity of this post-sweep procedure is minor part compared to the previous bottom-up fixing mechanism thus will not increase the order of our proposed algorithm. The pseudo-code of the proposed algorithm with bottom-up fixing mechanism is given in Fig. 2.13.

2.6 Simulation Results

In this section, we present simulation results for our proposed solution. The main goal is to demonstrate the performance of our algorithm.

2.6.1 Comparison Metric

Since our MILP problem is NP-hard in general [10], it is impractical to solve it via an optimization solver such as CPLEX within reasonable amount of time. Nevertheless, we can still run the problem in CPLEX solver; terminate the computation under a given (tolerable) time limit; and use the current (intermediate) lower bound obtained by the solver as a target for comparison. Obviously, such lower bound is likely to be very conservative and sets a high standard for our solution to measure up.

For ease of comparison, we will normalize our result w.r.t. the lower bound obtained by CPLEX. Note that the optimal solution (unknown) is between the solution obtained by our algorithm and the lower bound by CPLEX. Thus, if the normalized result is close to 1, then our solution must be even closer to the optimum.

2.6.2 Simulation Setting

For ease of scalability, we normalize all units for distance, bandwidth, power, rate with appropriate dimensions. We consider randomly generated ad hoc network topology consisting of 20, 30 and 40 nodes, respectively. For a 20 or 30-node network, the area of deployment is a 100×100 square whereas for a 40-node network, the area is 125×125. We assume $|\mathcal{B}| = 15$ and $W = 50$. The set of available bands at each node is randomly selected from the set of 15-band pool. The transmission power P is set to $4 \cdot 10^7 \eta$. The transmission range and the interference range are set to 30 and 50, respectively. The path loss index n is set to 4.

We assume there are $|\mathcal{L}| = 2$ multicast sessions for 20-node networks, and $|\mathcal{L}| = 3$ multicast

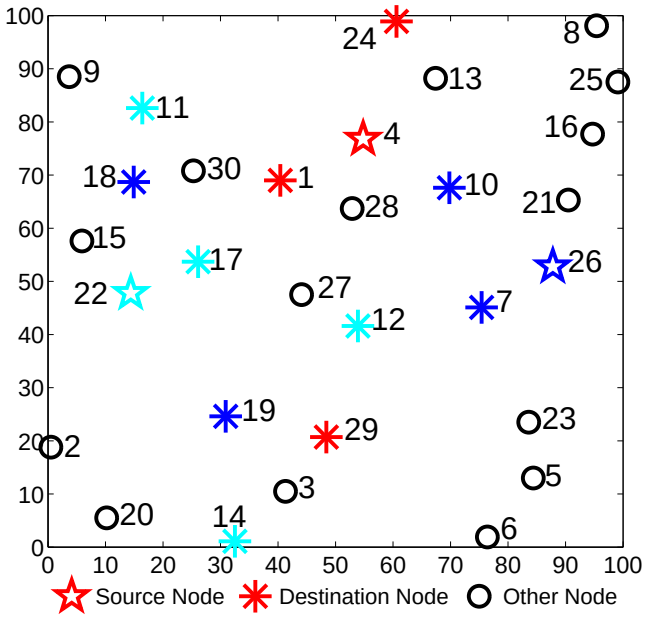

Figure 2.14: A 30-node CR ad hoc network used in the example.

sessions for 30 and 40-node networks. For each multicast session, the source node is randomly selected and the set of destination nodes is also randomly selected with a size within $[2, 5]$. The rate requirement for each session is randomly chosen within $[40, 100]$.

2.6.3 An Example

In the following section (Section 2.6.4), we will present 150 sets of results for randomly generated 20-, 30-, and 40-node networks. Before we present all those results, we will look into one instance of such result and gain some insights. The particular instance that we will examine is a 30-node network shown in Fig. 2.14, where pentacles represent source nodes, stars represent destination nodes, and circles represent other nodes in the network. Table 2.2 specifies the source nodes, the set of destination nodes for each source, and rate requirement for each session in the network. The location and available bands of each node are listed in Table 2.3.

Table 2.2: Source node, destination nodes, and rate requirement of each session in the example 30-node network.

Source Node	Destination Nodes	Rate Requirement
4	1,24,29	43
22	11,12,14,17	46
26	7,10,18,19	87

Table 2.3: Each node's location and available frequency bands for the example 30-node network.

Node	Location	Available Bands	Node	Location	Available Bands
1	(40.4, 69)	3,4,5,6,9,10,11,13,14	16	(94.7, 77.7)	1,7,9,12,14,15
2	(0.5, 18.8)	1,15	17	(26.1, 53.7)	2,3,4,5,6,7,10,13,14
3	(41.3, 10.5)	3,7,8,10,11,12,13	18	(14.9, 68.7)	2,3,4,5,6,13,14
4	(54.8, 76.8)	4,5,6,9,11,12,14,15	19	(30.9, 24.6)	2,3,7,8,10,11,12,13,15
5	(84.4, 13)	1,2,4,5,9,10,11	20	(10.2, 5.5)	1,11,12,15
6	(76.4, 1.9)	1,5,8,9,10,11	21	(90.5, 65.3)	1,2,7,9,12,14,15
7	(75.4, 45.1)	1,2,3,4,9,12,13,14,15	22	(14.4, 47.8)	2,3,6,7,8,10,13
8	(95.4, 98.1)	7,15	23	(83.6, 23.5)	1,2,3,4,9,10,11,12,13,14,15
9	(3.7, 88.5)	3,6,13,14	24	(60.6, 98.9)	5,9,11,14
10	(69.8, 67.6)	1,3,4,5,7,9,12,14,15	25	(99.1, 87.5)	1,7,9,12,14,15
11	(16.4, 82.6)	3,5,6,13,14	26	(87.8, 52.8)	1,2,3,7,9,12,14,15
12	(53.9, 41.6)	1,3,4,7,10,11,13,14,15	27	(44.1, 47.5)	2,3,4,5,7,10,11,13,14
13	(67.4, 88.2)	1,4,5,7,9,12,14,15	28	(52.9, 63.7)	1,3,4,5,6,9,10,12,13,14,15
14	(32.5, 1.1)	3,7,8,11,12,13,15	29	(48.4, 20.7)	3,7,8,10,11,12,13,15
15	(5.9, 57.6)	2,3,6,8,13	30	(25.3, 70.8)	2,3,4,5,6,10,13,14

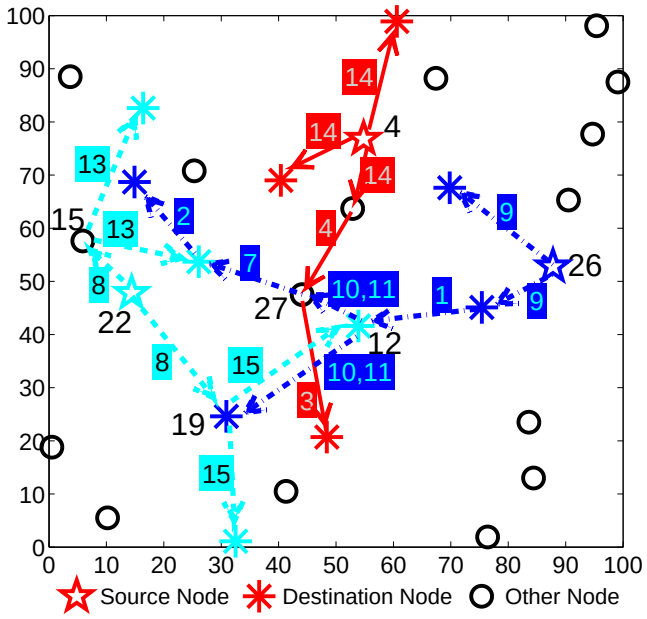

Figure 2.15: Solution for multicast sessions for the example 30-node CR ad hoc network.

The objective value obtained by our solution is 12, while the lower bound by CPLEX is also 12 for this instance. Thus, the normalized result is 1, indicating our solution happens to coincide with the optimal solution for this instance.

Figure 2.15 shows the details of our results. The numbers embedded in gray and over a link indicate the bands used for this transmission. As shown in the figure, WMA is employed on nodes 4, 12, 15, 19, 22, 26. Also note that since session 3 has a high rate requirement (87), one band is not adequate to support this multicast transmission from node 12 to both nodes 19 and 27. As a result, node 12 now uses two bands (10 and 11) to transmit data to node 19 (also broadcast to node 27).

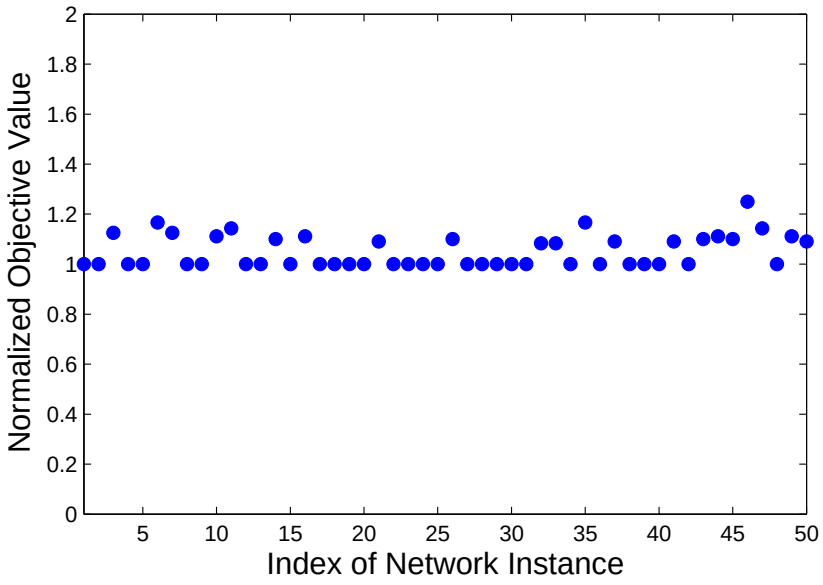

Figure 2.16: Results for 50 instances of 20-node CR ad hoc network.

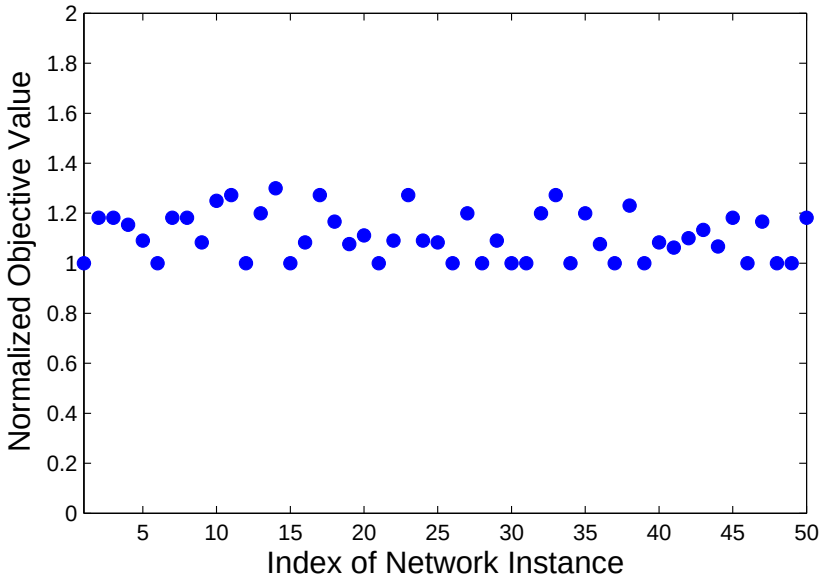

Figure 2.17: Results for 50 instances of 30-node CR ad hoc network.

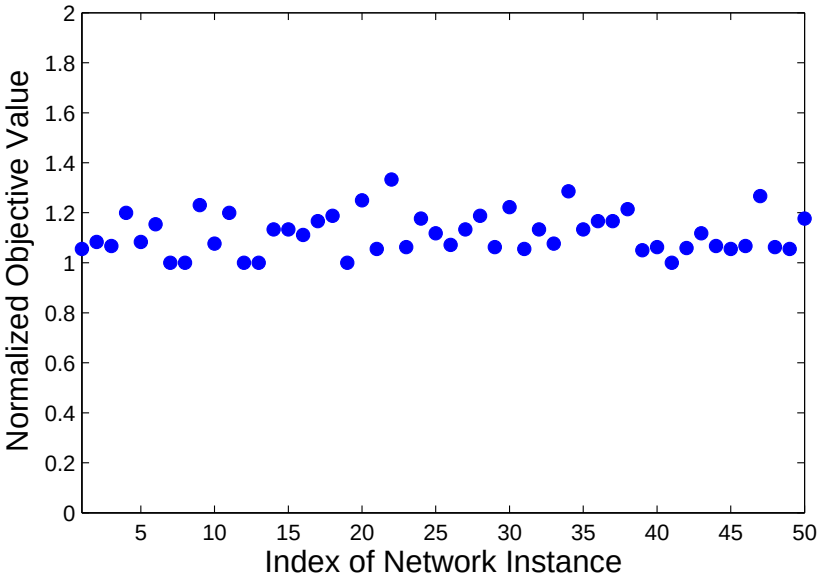

Figure 2.18: Results for 50 instances of 40-node CR ad hoc network.

2.6.4 Simulation Results on 150 CRNs

We now present complete results for 20-, 30-, and 40-node CR ad hoc networks. The results are shown in Figs. 2.16, 2.17 and 2.18, respectively. For each network size, we generate 50 network instances with different parameter settings (see Section 2.6.2) and run both our proposed solution and CPLEX optimization solver (to obtain a lower bound). In each figure, the x-axis gives the index for each network instance and the y-axis shows the normalized objective function (w.r.t. the lower bound obtained via CPLEX). Therefore, the normalize objective value is always be greater than or equal to 1. Given that the optimal solution must lie within our solution and the lower bound, the closer the normalize objective value to 1, the better the solution, with 1 being the case that the solution is optimal.

In Table 2.4, we list the mean and standard deviation of the normalized objective value for the 20-, 30-, and 40-node network, all with 50 simulation runs. For each network size, the mean is close to 1 and the standard deviation is small, indicating that the result from our proposed solution

Table 2.4: Average normalized objective value and standard deviation for 20-, 30-, and 40-node networks, each run over 50 network instances.

Network Size	Average Normalized Objective	Standard Deviation
20-node	1.050	0.064
30-node	1.111	0.095
40-node	1.117	0.082

is very close to the lower bound obtained by CPLEX. In many cases, the solution by our algorithm is identical to the lower bound, which means that the solution coincides with optimum. Since the optimal solution is between our result and our lower, we conclude that our proposed solution is very close to optimal and thus is highly competitive.

2.7 Conclusion

Given the wide acceptance of CR for future wireless communications, in this chapter, we studied multicast communication problem in an ad hoc network where each node is equipped with a CR. The goal is to minimize the required network resource to support a set of multicast sessions, with each multicast session associated with a given flow rate. We showed that the unique characteristics associated with CR make this problem much more complex and difficult than that for an ad hoc network based on traditional hardware-based radio. We formulated the resource optimization problem into a mixed integer linear program (MILP) via a cross-layer approach. We developed a polynomial time algorithm that incorporates several novel ideas such as identification of key integer variables, fixing these variables via a series of relaxed linear programming, and tying up such integer fixing with a bottom-up tree construction. Based on simulation results, we showed that the proposed algorithm offers highly competitive solution, based on its closeness to a lower bound.

Chapter 3

Joint Optimization of MIMO and Cognitive Radio Networks

3.1 Introduction

In parallel to the development of CR for DSA, MIMO [4, 45] has widely been accepted and now implemented in commercial wireless products to increase capacity. The goal of MIMO and how it operates are largely independent and orthogonal to CR. Instead of exploiting idle channels for wireless communications, MIMO attempts to increase capacity within the same channel via space-time processing [14]. In particular, by employing multiple antennas on both the transmitting and receiving nodes, wireless channel capacity can scale almost linearly with the number of antennas (via spatial multiplexing) [9, 43]. Further, with zero-forcing beamforming (ZFBF) [5, 47], a node may uses its degrees of freedom to mitigate interference from other nodes or its own interference to other nodes.

Currently, the advances of CR (see, e.g., [16, 19, 30, 32, 35, 39, 41]) and MIMO (see, e.g., [3, 7, 15, 21–24, 40, 42, 44]) are largely independent and parallel to each other. CR operates on the channel/band level to exploit efficiency across spectrum dimension while MIMO operates within

the same channel to exploit efficiency within the same band. Recognizing the joint potential of CR (across spectrum bands) and MIMO (within the same spectrum band), S. Haykin pointed out that "... it seems logical to explore building the MIMO antenna architecture in the design of cognitive radio. The end-result is a cognitive MIMO radio that offers the ultimate in flexibility" [17].

Assuming that CR and MIMO will ultimately marry each other and offer the ultimate flexibility in DSA and spectrum efficiency, we would like to inquire the potential capacity gain in this marriage. In particular, we are interested in how such marriage will affect capacity of a user communication session in a *multi-hop* CRN. If we assume that each node in a CRN is equipped with A_{MIMO} antennas, then one would expect at least A_{MIMO}-fold capacity increase when compared to a CRN with only a single antenna at each node, due to spatial multiplexing gain from MIMO. Now observing that CR and MIMO handle interference differently (with CR from channel level and MIMO within a channel), we ask the following fundamental question: *Will joint optimization of CR (via channel assignment) and MIMO (via DoF allocation) offers more than A_{MIMO}-fold capacity increase?*

In this chapter, we investigate this fundamental problem. The answer to this question is important as it will show whether or not joint optimization of both technologies is necessary, given that one already can have A_{MIMO}-fold capacity increase by using MIMO spatial multiplexing. We consider a multi-hop MIMO-empowered CR network, which we call CRN^{MIMO}. We develop a tractable mathematical model for CRN^{MIMO}, which captures the essence of channel assignment (for CR) and DoF allocation (for MIMO). We formulate this joint optimization problem into a mathematical program with the goal of maximizing the minimum rate among user sessions. Then, based on this mathematical model, we use numerical results to show how channel assignment in CRN and DoF allocation in MIMO can be jointly optimized to maximize capacity. We give an affirmative answer that the joint optimization of CR and MIMO can offer *more than* A_{MIMO}-fold capacity increase for a CRN with only a single antenna at each node.

The remainder of this chapter is organized as follows. In Section 3.2, we offer some basic understanding of CR and MIMO, thus laying the foundation for mathematical modeling. In Sec-

tion 3.3, we present mathematical models for joint optimization of CR and MIMO. In Section 3.4, we present numerical results and validate the capacity increase with joint optimization. Section 3.5 concludes this chapter.

3.2 Understanding CRN^{MIMO}

In this section, we review some important characteristics associated with MIMO-empowered CRN, or CRN^{MIMO}. First, on channel level, the CRNs exploit available spectrum and handle interference via the use of different channels, as we discussed in Section 2.3.1. Second, within a channel, MIMO mitigate co-channel interference via ZFBF (i.e., using DoF), as we will discuss in the following section. A thorough understanding of these interference avoidance/cancellation techniques across/within channels is critical to mathematical modeling and ultimately fully exploit the potential of CRN^{MIMO}.

3.2.1 Co-Channel Interference Cancellation with MIMO DoFs

Complementary to a CR's ability to handle interference at the channel level, MIMO can further mitigate potential interference within a channel (band). The total number of antennas at a node is called *degrees of freedom* (or DoFs) [36] at the node. A node can use some or all of its DoFs for either spatial multiplexing (to achieve multiple concurrent data streams over a link) or co-channel interference cancellation (to enable multiple links on the same band), as long as the number of DoFs being used does not exceed the number of antennas at the node.

The allocation of DoFs at a node for data transmission or interference cancellation depends on how the nodes in the network are "ordered". The significance of such ordering will be discussed late in this section. For a given ordered node list, the DoFs at a node can be allocated as follows.

- *Transmitting Node Behavior.* First, the transmitting node needs to allocate DoFs for data transmission. The number of DoFs to be allocated equals to the number of data streams to be

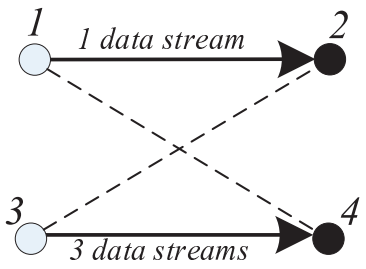

Figure 3.1: DoF allocation in MIMO.

transmitted. Then, for interference cancellation, this node must ensure that its transmission does not interfere with those receiving nodes that are before this node in the ordered list. To cancel its interference to these receiving nodes, this node needs to allocate a number of DoFs that is equal to the received data streams by those nodes. This transmitting node does not need to allocate any of its DoFs to null potential interference to those receiving nodes that are after itself in the ordered node list.

- *Receiving Node Behavior.* First, the receiving node needs to allocate DoFs for data reception. The number of DoFs to be allocated equals to the number of data streams to be received. Then, for interference cancellation, this node must ensure that its reception is not interfered by those transmitting nodes that are ordered before this node in the list. To cancel the interference from these transmitting nodes, this node needs to allocate a number of DoFs that is equal to the transmitted data streams by those nodes. This node does not need to allocate any of its DoFs to null potential interference from those transmitting nodes that are after itself in the ordered node list.

An example is given in Fig. 3.1, where there are four nodes, each equipped with four antennas. All nodes operate on the same band and there are two mutually interfering links in the network: $1 \rightarrow 2$ and $3 \rightarrow 4$. Suppose the ordered node list is 1, 2, 3, and 4. Further, node 1 is transmitting to node 2 with 1 data stream. Now we show how the DoFs at each node are allocated for interference cancellation and spatial multiplexing.

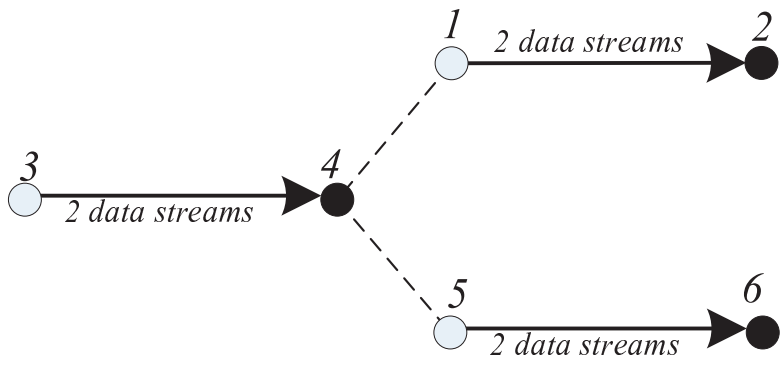

Figure 3.2: A 6-node 3-link example illustrating the importance of node ordering in DoF allocation.

- Starting with node 1, it is the first node in the list and it is a transmitting node. Then it allocates 1 DoF for its transmission with 1 data stream. It does not need to allocate any DoF to cancel potential interference to other receiving nodes that are after itself in the ordered node list, i.e., node 4.
- The next node in the list is node 2. As a receiving node, it allocates 1 DoF for receiving 1 data stream from node 1. It does not need to consider allocating any DoF to mitigate interference from other transmitting nodes that are after itself in the ordered node list, i.e., node 3.
- The next node in the list is node 3. As a transmitting node, it needs to ensure that its transmission does not interfere with any receiving node before itself in the list, i.e., node 2. Thus, node 3 uses 1 DoF (equals to the number of received data streams by node 2) to cancel its interference on node 2. Now it has 3 remaining DoFs, which can all be used to transmit data streams (up to 3) to node 4.
- The last node in the list is node 4. As a receiving node, node 4 needs to allocate 3 of its DoFs for receiving 3 data streams from node 3. Node 4 also needs to use its remaining 1 DoF (equals to the number of transmitted data streams by node 1) to cancel interference from node 1. This completes the DoF allocation at each node.

Why Ordering Is Important The above example for DoF allocation in Fig. 3.1 is for a given

node order of 1, 2, 3, and 4. Now we show that the ordering of nodes in DoF allocation is important, in the sense that an ordering directly affects the final solution. This affirms that finding an optimal ordering should be part of the problem formulation.

The importance of node ordering for DoF allocation is best explained with an example. Consider a 6-node 3-link example in Fig. 3.2, where links $1 \rightarrow 2$, $3 \rightarrow 4$ and $5 \rightarrow 6$ all operate on the same band. The interference relationship is indicated as dashed line, i.e., both nodes 1 and 5 interfere node 4. There are four antennas at each node. The goal is to transmit 2 data streams on each of these 3 links. We now show that different node ordering will lead to different result.

- **Node Order:** 1**,** 3**,** 5**,** 4**,** 2 **and** 6**.** Starting with node 1, it is the first node in the list and it is a transmitting node. Then it allocates 2 DoFs to transmit 2 data streams to node 2. The next node in the list is node 3. As a transmitting node, it allocates 2 DoFs to transmit 2 data streams to node 4. The next node in the list is node 5. As a transmitting node, it allocates 2 DoFs to transmit 2 data streams to node 6. The next node in the list is node 4. It needs to cancel interference from transmitting nodes before itself in the list, i.e., node 1 and node 5. For each of these transmitting nodes, node 4 needs to allocate 2 DoFs. Now node 4 has already used up all 4 of its DoFs. But for receiving 2 data streams from node 3, node 4 needs to allocate another 2 DoFs. Thus, under this node ordering list, DoF allocation to achieve 2 data streams on each link is not feasible.

- **Node Order:** 1**,** 2**,** 4**,** 3**,** 6 **and** 5**.** Now consider this node ordering for DoF allocation. Starting with node 1, it is the first node in the list and it is a transmitting node. Then it allocates 2 DoFs to transmit 2 data streams to node 2. The next node in the list is node 2. As a receiving node, node 2 allocates 2 DoFs for receiving 2 data streams from node 1. The next node in the list is node 4. As a receiving node, node 4 needs to allocate 2 of its DoFs for receiving 2 data streams from node 3. Node 4 also needs to use its remaining 2 DoF to cancel interference from node 1, which is before itself in the node list. The next node in the list is node 3. As a transmitting node, node 3 allocates 2 DoFs to transmit 2 data streams to node 4. The next node in the list is node 6. As a receiving node, node 6 needs to allocate 2

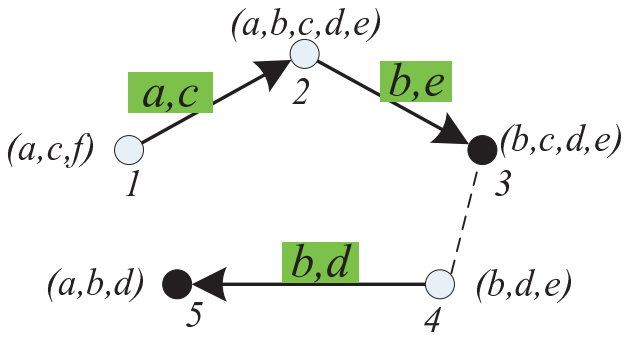

Figure 3.3: An example of CRN$^{\text{MIMO}}$.

of its DoFs for receiving 2 data streams from node 5. The last node in the list is node 5. As a transmitting node, node 5 needs to ensure that its transmission does not interfere with any receiving node before itself in the list, i.e., node 4. Thus node 5 uses 2 DoFs to cancel its interference on node 4. Now it has 2 remaining DoFs, which it uses to transmit 2 data streams to node 6. This completes the DoF allocation at each node. Now we have a feasible DoF allocation under this node ordering list.

The above two examples show the importance of node ordering in DoF allocation. Consequently, such node ordering must be part of the formulation in our optimization problem.

3.2.2 An Example of CRN$^{\text{MIMO}}$

We now offer an example to illustrate how interference is jointly handle at channel level (via CR) and within a channel (via MIMO). Figure 3.3 shows a 5-node CRN$^{\text{MIMO}}$ with each node equipped with four antennas. The available bands at nodes 1 to 5 are $\{a, c, f\}$, $\{a, b, c, d, e\}$, $\{b, c, d, e\}$, $\{b, d, e\}$, and $\{a, b, d\}$, respectively. There are two communication sessions in the network, i.e., $1 \rightarrow 2 \rightarrow 3$ and $4 \rightarrow 5$. The usable bands on links $1 \rightarrow 2$, $2 \rightarrow 3$, and $4 \rightarrow 5$ are $\{a, c\}$, $\{b, c, d, e\}$, and $\{b, d\}$, respectively.

Suppose our objective is to maximize the minimum rate for sessions $1 \rightarrow 2 \rightarrow 3$ and $4 \rightarrow 5$.

The mathematical formulation for such type of problems will be presented in the next section. It can be shown that by solving the optimization problem, 6 data streams can be transported on each of the two sessions. An optimal band usage on each link and DoF allocation at each node is the following. On link $1 \rightarrow 2$, bands a and c are used, where on band a, node 1 allocates 4 DoFs for transmitting 4 data streams to node 2; and on band c, node 1 allocates 2 DoFs for transmitting 2 data streams to node 2. Correspondingly, on band a, node 2 allocates 4 DoFs for receiving 4 data streams from node 1; and on band c, node 2 allocates 2 DoFs for receiving 2 data streams from node 1. On link $2 \rightarrow 3$, bands b and e are used, where on band b, node 2 allocates 2 DoFs for transmitting 2 data streams to node 3; and on band e, node 2 allocates 4 DoFs for transmitting 4 data streams to node 3. Correspondingly, at node 3, on band b, 2 DoFs are allocated for receiving 2 data streams from node 2; and on band e, node 3 allocates 4 DoFs for receiving 4 data streams from node 2. On link $4 \rightarrow 5$, bands b and d are used. Node 4 first allocates 2 DoFs for transmitting 2 data streams to node 5 on band b. Since node 3 is also active on band b thus will be interfered, and the ordered node list on band b is 2, 3, 4, 5, node 4 thus allocates the remaining 2 DoFs on band b to cancel its interference to node 3. On band d, node 4 allocates 4 DoFs for transmitting 4 data streams to node 5. Correspondingly, at node 5, on band b, 2 DoFs are allocated for receiving 2 data streams from node 4; and on band d, node 5 allocates 4 DoFs for receiving 4 data streams from node 4.

It is important to realize that a node's DoFs are available for allocation on each channel. The use of DoF for interference cancellation and spatial multiplexing only has significance within the same channel. Given that there are multiple bands at each node and that there are DoFs within each band, the potential optimization space for capacity is large. In fact, we shall show that the optimal solution under CRN$^{\text{MIMO}}$ is greater than the number of antennas at each node (assuming same number at each node) multiplies the solution under a CRN (without MIMO). For example, it is easy to verify that for the later network (i.e., a CRN without MIMO), one of the two sessions in Fig. 3.3 can only have a rate of 1 data stream. Comparing to 6 data streams under CRN$^{\text{MIMO}}$, we have 6 (> 4) folds increase in minimum session rate. This result will be further discussed in Section 3.3 and substantiated in numerical results (Section 3.4).

3.3 Mathematical Modeling

3.3.1 Modeling of CRN$^{\text{MIMO}}$

We consider a CRN$^{\text{MIMO}}$ consisting of a set of $\mathcal{N}$ nodes. At each node $i \in \mathcal{N}$, there is a set of $\mathcal{B}_i$ available frequency bands that can be used for communications. As discussed, $\mathcal{B}_i$ may represent the set of bands that are unused by primary users and may be different at each node due to geographical difference. Denote the set of commonly available bands between nodes i and j as $\mathcal{B}_{ij} = \mathcal{B}_i \bigcap \mathcal{B}_j$. Also, denote A_i as the number of antennas at node i.

Suppose there are multiple sessions in this network. Denote $\mathcal{Q}$ the set of all sessions in the network. For a session $q \in \mathcal{Q}$, denote $s(q)$ the source node, $d(q)$ the destination node, and $f(q)$ the flow rate (in b/s). Table 3.1 lists all notation used in this chapter.

To model the half-duplex nature of each node on a band, we use two binary variables g_i^b and h_i^b to indicate node i's transmission/reception status on band b, i.e.,

$$g_i^b = \begin{cases} 1 & \text{if node } i \text{ is transmitting on band } b, \\ 0 & \text{otherwise.} \end{cases} \qquad (i \in \mathcal{N}, b \in \mathcal{B}_i)$$

$$h_i^b = \begin{cases} 1 & \text{if node } i \text{ is receiving on band } b, \\ 0 & \text{otherwise.} \end{cases} \qquad (i \in \mathcal{N}, b \in \mathcal{B}_i)$$

Then the half-duplex constraint (i.e., a node cannot transmit and receive at the same time on the same band) can be represented as follows.

$$g_i^b + h_i^b \leq 1 \qquad (i \in \mathcal{N}, b \in \mathcal{B}_i)\ . \tag{3.1}$$

As we discussed in Section 3.2.1, on any given band, the total number of data streams for transmission or reception at a node is limited by its number of antennas. Denote l as a link in the network and z_l^b as the number of data streams over link l on band b. Then we have the following

Table 3.1: Notation in Chapter 3

Symbol	Definition
A_i	The number of antennas at node $i \in \mathcal{N}$
A_{MIMO}	The number of antennas at each node (when each node has the same number of antennas)
$\mathcal{B}_i$	The set of available bands at node $i \in \mathcal{N}$
$\mathcal{B}_{ij}$	The set of common available bands at nodes $i, j \in \mathcal{N}$
c	The capacity when one DoF is used for data transmission on a band over a link
$d(q)$	Destination node of session q
$f(q)$	The rate of session q
g_i^b	A binary indicator. g_i^b is 1 if node i is transmitting, or 0 otherwise.
h_i^b	A binary indicator. h_i^b is 1 if node i is receiving, or 0 otherwise.
$\mathcal{I}_i^b$	The set of nodes in the interference range of node i on band b
$\mathcal{L}_{i,b}^{\text{Out}}$	The set of outgoing links on band b at node i
$\mathcal{L}_{i,b}^{\text{In}}$	The set of incoming links on band b at node i
$\mathcal{L}_{\text{Active}}$	The set of links used for routing
$\mathcal{N}$	The set of all nodes in the network
$\mathcal{Q}$	The set of active sessions in the network
$\text{Rx}(l)$	Receiving node of link l
$s(q)$	Source node of session q
$\text{Tx}(l)$	Transmitting node of link l
z_l^b	The number of data streams over link l on band b
θ_{ji}^b	Binary indicator showing the relationship between nodes i and j in the ordered list on band b
λ_{ji}^b	The number of DoFs on band b used by transmitting node i to cancel its interference to node j
μ_{ji}^b	The number of DoFs on band b used by receiving node i to cancel the interference from node j

two constraints.

$$g_i^b \leq \sum_{l \in \mathcal{L}_{i,b}^{\text{Out}}} z_l^b \leq g_i^b A_i \qquad (i \in \mathcal{N}, b \in \mathcal{B}_i) \ , \tag{3.2}$$

$$h_i^b \leq \sum_{l \in \mathcal{L}_{i,b}^{\text{In}}} z_l^b \leq h_i^b A_i \qquad (i \in \mathcal{N}, b \in \mathcal{B}_i) \ , \tag{3.3}$$

where $\mathcal{L}_{i,b}^{\text{Out}}$ and $\mathcal{L}_{i,b}^{\text{In}}$ represent the sets of outgoing and incoming links at node i on band b, respectively.

As discussed in Section 3.2.1, the DoF allocation (for transmission/reception and interference cancellation) at each node is determined sequentially based on an ordered node list. This ordering directly affects DoF allocation in the final solution and should be part of the optimization problem. To model the ordering relationship among the nodes, we define the following variable.

$$\theta_{ji}^b = \begin{cases} 1 & \text{Node } i \text{ is after node } j \text{ in the node list on band } b, \\ 0 & \text{Node } i \text{ is before node } j \text{ in the node list on band } b. \end{cases} \qquad (i, j \in \mathcal{N}, j \neq i, b \in \mathcal{B}_{ij})$$

Based on the definition of θ-variable, we have

$$\theta_{ji}^b + \theta_{ij}^b = 1 \quad (i, j \in \mathcal{N}, b \in \mathcal{B}_{ij}) \ . \tag{3.4}$$

Also, the transitivity property should hold for the θ-variables. That is, for any three nodes i, j and k on band b, if node i is after node j and node j is after node k (i.e., $\theta_{ji}^b = 1$ and $\theta_{kj}^b = 1$), then node i is after node k (i.e., $\theta_{ki}^b = 1$). This transitivity can be formulated by the following two inequalities.

$$\theta_{kj}^b + \theta_{ji}^b - 1 \leq \theta_{ki}^b \leq \theta_{kj}^b + \theta_{ji}^b \quad (i, j, k \in \mathcal{N}, b \in \mathcal{B}_i \bigcap \mathcal{B}_j \bigcap \mathcal{B}_k) \ .$$

The correctness of the above two inequalities can be easily verified by trying out all possible sums of θ_{kj}^b and θ_{ji}^b and comparing with possible values of θ_{ki}^b. Note that by (3.4), we have $\theta_{ki}^b = 1 - \theta_{ik}^b$, then the above two inequalities can be rewritten in the following form.

$$1 \leq \theta_{ik}^b + \theta_{kj}^b + \theta_{ji}^b \leq 2 \qquad (i, j, k \in \mathcal{N}, b \in \mathcal{B}_i \bigcap \mathcal{B}_j \bigcap \mathcal{B}_k) \ . \tag{3.5}$$

Now we consider DoF allocation at a node, which includes DoFs allocated for transmission/reception and DoFs allocated for interference cancellation. For transmission and reception,

the number of required DoFs are $\sum_{l\in\mathcal{L}_{i,b}^{\text{Out}}} z_l^b$ for a transmitting node i and $\sum_{m\in\mathcal{L}_{j,b}^{\text{In}}} z_m^b$ for a receiving node j, respectively. For interference cancellation, as discussed in Section 3.2.1, a transmitting node needs to allocate its DoFs to cancel its interference to all receiving nodes before itself in the ordered node list. Denote $\mathcal{I}_i^b$ the set of nodes to which node i can interfere on band b. Then the number of DoFs that node i allocates for interference cancellation can be computed as $\sum_{j\in\mathcal{I}_i^b}(\theta_{ji}^b \cdot \sum_{m\in\mathcal{L}_{j,b}^{\text{In}}}^{\text{Tx}(m)\neq i} z_m^b)$, where the inner summation $\sum_{m\in\mathcal{L}_{j,b}^{\text{In}}}^{\text{Tx}(m)\neq i} z_m^b$ gives the number of data streams for a given receiving node j while the outer summation is taken only over those receiving nodes that are before node i in the ordered node list. Now considering both the DoFs at a node allocated for transmission and interference cancellation, we have the following constraint.

$$\sum_{l\in\mathcal{L}_{i,b}^{\text{Out}}} z_l^b + \sum_{j\in\mathcal{I}_i^b}\left(\theta_{ji}^b \cdot \sum_{m\in\mathcal{L}_{j,b}^{\text{In}}}^{\text{Tx}(m)\neq i} z_m^b\right) \leq A_i g_i^b + (1-g_i^b)M \qquad (i\in\mathcal{N}, b\in\mathcal{B}_i)\ , \tag{3.6}$$

where M is a sufficiently large number to ensure the constraint holds when node i is not a transmitting node (e.g., we can set $M = \sum_{j\in\mathcal{I}_i^b} A_j$). Similarly, if node i is a receiving node, we have the following constraint for its DoF allocation.

$$\sum_{l\in\mathcal{L}_{i,b}^{\text{In}}} z_l^b + \sum_{j\in\mathcal{I}_i^b}\left(\theta_{ji}^b \cdot \sum_{m\in\mathcal{L}_{j,b}^{\text{Out}}}^{\text{Rx}(m)\neq i} z_m^b\right) \leq A_i h_i^b + (1-h_i^b)M \qquad (i\in\mathcal{N}, b\in\mathcal{B}_i)\ . \tag{3.7}$$

For a given route for each session, we can identify the set of links on this route. Denote $\mathcal{L}_{\text{Active}}$ the set of links that are used by all these routes in the network. Then we have the following capacity constraint on link $l\in\mathcal{L}_{\text{Active}}$.

$$\sum_{q\in\mathcal{Q}}^{l \text{ is traversed by } q} f(q) \ \leq\ c\cdot \sum_{b\in\mathcal{B}_{\text{Tx}(l),\text{Rx}(l)}} z_l^b \qquad (l\in\mathcal{L}_{\text{Active}})\ , \tag{3.8}$$

where $f(q)$ is the flow rate of session $q\in\mathcal{Q}$ and c is the capacity when one DoF is used for data transmission on a band over link l.

For the CRN$^{\text{MIMO}}$ under investigation, suppose we want to maximize the minimum capacity

among the sessions, then the optimization problem (denoted as OPT) can be formulated as follows.

$$
\begin{aligned}
\textbf{(OPT)} \qquad & \max \quad && f_{\min} && \\
& \text{s.t.} && f_{\min} \leq f(q) && (q \in \mathcal{Q}) \\
& && \text{Constraints } (3.1)\text{–}(3.8) && \\
& && f_{\min}, f(q) \geq 0 && (q \in \mathcal{Q}) \\
& && g_i^b, h_i^b \in \{0,1\} && (i \in \mathcal{N}, b \in \mathcal{B}_i) \\
& && z_l^b \geq 0 && (l \in \mathcal{L}_{\text{Active}}, b \in \mathcal{B}_{\text{Tx}(l),\text{Rx}(l)}) \\
& && \theta_{ji}^b \in \{0,1\} && (i,j \in \mathcal{N}, j \neq i, b \in \mathcal{B}_{ij}) \ .
\end{aligned}
$$

In this formulation, $f_{\min}$, $f(q)$, g_i^b, h_i^b, z_l^b, and θ_{ji}^b are optimization variables and A_i, M and c are given constants. Due to the nonlinear product term $\sum_{j \in \mathcal{I}_i^b}(\theta_{ji}^b \cdot \sum_{m \in \mathcal{L}_{j,b}^{\text{In}}}^{\text{Tx}(m)\neq i} z_m^b)$ in (3.6), $\sum_{j \in \mathcal{I}_i^b}(\theta_{ji}^b \cdot \sum_{m \in \mathcal{L}_{j,b}^{\text{Out}}}^{\text{Rx}(m)\neq i} z_m^b)$ in (3.7), and integer variables, the problem is in the form of Mixed Integer Non-Linear Programming (MINLP).

3.3.2 Mathematical Reformulation

A closer examination of our formulation in the last section shows that it can be made more compact and simpler (e.g., removal of redundant constraints and nonlinear terms). In this section, we give details in this direction.

Removing Redundancy. There are 6 permutations for any set of three nodes $\{u, v, w\}$, where $\{u, v, w\} \subset \mathcal{N}$. Note that according to (3.5), we can write 12 different constraints in 6 groups for any band $b \in \mathcal{B}_u \bigcap \mathcal{B}_v \bigcap \mathcal{B}_w$ as follows. By letting $i = u$, $j = w$, $k = v$ in (3.5), we have

$$1 \leq \theta_{uv}^b + \theta_{vw}^b + \theta_{wu}^b \leq 2 \ . \tag{3.9}$$

By letting $i = u$, $j = v$, $k = w$ in (3.5), we have

$$1 \leq \theta_{uw}^b + \theta_{wv}^b + \theta_{vu}^b \leq 2 \ . \tag{3.10}$$

Follow the same token, we list the other 4 groups as follows.

$$1 \leq \theta^b_{vw} + \theta^b_{wu} + \theta^b_{uv} \leq 2 \ , \tag{3.11}$$

$$1 \leq \theta^b_{wv} + \theta^b_{vu} + \theta^b_{uw} \leq 2 \ , \tag{3.12}$$

$$1 \leq \theta^b_{vu} + \theta^b_{uw} + \theta^b_{wv} \leq 2 \ , \tag{3.13}$$

$$1 \leq \theta^b_{wu} + \theta^b_{uv} + \theta^b_{vw} \leq 2 \ . \tag{3.14}$$

A closer look at these 6 groups of constraints shows that (3.9), (3.11), (3.14) are the same; (3.10), (3.12), (3.13) are the same. That is, we only need (3.9) and (3.10) for any set of three nodes $\{u, v, w\}$. Further, it is easy to verify that (3.9) is equal to (3.10) since $\theta^b_{uv} = 1-\theta^b_{vu}$, $\theta^b_{vw} = 1-\theta^b_{wv}$, and $\theta^b_{wu} = 1 - \theta^b_{uw}$ by (3.4).

To conclude, for any set of three nodes $\{i, j, k\}$, the following constraints are sufficient to describe the transitivity property.

$$1 \leq \theta^b_{ik} + \theta^b_{kj} + \theta^b_{ji} \leq 2 \quad (\{i, j, k\} \subset \mathcal{N}, b \in \mathcal{B}_i \bigcap \mathcal{B}_j \bigcap \mathcal{B}_k) \ . \tag{3.15}$$

It is not hard to see that the number of constraints in (3.15) is only $\frac{1}{6}$ of that in (3.5). Thus by using (3.15) instead of (3.5), we can significantly reduce redundancy in our problem formulation.

Linearization. Note that the constraints in (3.6) and (3.7) have nonlinear terms (product of variables), which bring in extra complexity in problem formulation. We now show how these nonlinear terms can be removed via linearization. For the nonlinear term in (3.6), we define a new variable λ^b_{ji} as follows.

$$\lambda^b_{ji} = \theta^b_{ji} \cdot \sum_{m \in \mathcal{L}^{\text{In}}_{j,b}}^{\text{Tx}(m) \neq i} z^b_m \qquad (i \in \mathcal{N}, b \in \mathcal{B}_i, j \in \mathcal{I}^b_i) \ , \tag{3.16}$$

which is the number of DoFs that transmitting node i uses to cancel the interference to receiving node j. With λ^b_{ji}, (3.6) can be rewritten as:

$$\sum_{l \in \mathcal{L}^{\text{Out}}_{i,b}} z^b_l + \sum_{j \in \mathcal{I}^b_i} \lambda^b_{ji} \leq A_i g^b_i + (1 - g^b_i) M \qquad (i \in \mathcal{N}, b \in \mathcal{B}_i) \ . \tag{3.17}$$

Now, we need to add some constraints for λ_{ji}^b. This can be done by examining the definition of λ_{ji}^b in (3.16). For binary variable θ_{ji}^b, we have the following relaxed constraints: $\theta_{ji}^b \geq 0$, $1-\theta_{ji}^b \geq 0$. For $\sum_{m\in\mathcal{L}_{j,b}^{\text{In}}}^{\text{Tx}(m)\neq i} z_m^b$, we have: $\sum_{m\in\mathcal{L}_{j,b}^{\text{In}}}^{\text{Tx}(m)\neq i} z_m^b \geq 0$, $A_j - \sum_{m\in\mathcal{L}_{j,b}^{\text{In}}}^{\text{Tx}(m)\neq i} z_m^b \geq 0$. Multiplying each constraint involving θ_{ji}^b by one of the two constraints involving $\sum_{m\in\mathcal{L}_{j,b}^{\text{In}}}^{\text{Tx}(m)\neq i} z_m^b$, and replacing the product term $\theta_{ji}^b \cdot \sum_{m\in\mathcal{L}_{j,b}^{\text{In}}}^{\text{Tx}(m)\neq i} z_m^b$ with the new variable λ_{ji}^b, we obtain the following four constraints.

$$\lambda_{ji}^b \geq 0 \qquad (i\in\mathcal{N}, b\in\mathcal{B}_i, j\in\mathcal{I}_i^b)\ , \tag{3.18}$$

$$\lambda_{ji}^b \leq \sum_{m\in\mathcal{L}_{j,b}^{\text{In}}}^{\text{Tx}(m)\neq i} z_m^b \qquad (i\in\mathcal{N}, b\in\mathcal{B}_i, j\in\mathcal{I}_i^b)\ , \tag{3.19}$$

$$\lambda_{ji}^b \leq A_j\cdot\theta_{ji}^b \qquad (i\in\mathcal{N}, b\in\mathcal{B}_i, j\in\mathcal{I}_i^b)\ , \tag{3.20}$$

$$\lambda_{ji}^b \geq A_j\cdot\theta_{ji}^b - A_j + \sum_{m\in\mathcal{L}_{j,b}^{\text{In}}}^{\text{Tx}(m)\neq i} z_m^b \qquad (i\in\mathcal{N}, b\in\mathcal{B}_i, j\in\mathcal{I}_i^b)\ . \tag{3.21}$$

Note that due to the relaxation of integer variable θ_{ji}^b, $\sum_{m\in\mathcal{L}_{j,b}^{\text{In}}}^{\text{Tx}(m)\neq i} z_m^b$, and product operations, the above four constraints for λ_{ji}^b might be looser than (3.16). However, for the special case when θ_{ji}^b is a binary variable, it can be easily verified that (3.16) is equivalent to the four constraints in (3.18)–(3.21). Therefore, it is sufficient to have linear constraints (3.17)–(3.21) to replace (3.6).

Similarly, to remove the nonlinear term in (3.7), we define μ_{ji}^b as the number of DoFs that receiving node i uses to cancel the interference from transmitting node j. Following the same token, (3.7) can be replaced by the following linear constraints.

$$\sum_{l\in\mathcal{L}_{i,b}^{\text{In}}} z_l^b + \sum_{j\in\mathcal{I}_i^b}\mu_{ji}^b \leq A_i h_i^b + (1-h_i^b)M \qquad (i\in\mathcal{N}, b\in\mathcal{B}_i)\ ,$$

$$\mu_{ji}^b \geq 0 \qquad (i\in\mathcal{N}, b\in\mathcal{B}_i, j\in\mathcal{I}_i^b)\ ,$$

$$\mu_{ji}^b \leq \sum_{m\in\mathcal{L}_{j,b}^{\text{Out}}}^{\text{Rx}(m)\neq i} z_m^b \qquad (i\in\mathcal{N}, b\in\mathcal{B}_i, j\in\mathcal{I}_i^b)\ ,$$

$$\mu_{ji}^b \leq A_j\cdot\theta_{ji}^b \qquad (i\in\mathcal{N}, b\in\mathcal{B}_i, j\in\mathcal{I}_i^b)\ ,$$

$$\mu_{ji}^b \geq A_j\cdot\theta_{ji}^b - A_j + \sum_{m\in\mathcal{L}_{j,b}^{\text{Out}}}^{\text{Rx}(m)\neq i} z_m^b \qquad (i\in\mathcal{N}, b\in\mathcal{B}_i, j\in\mathcal{I}_i^b)\ .$$

Summary. With the above redundancy removal and linearization, we have a revised optimization

problem formulation (denoted as OPT-R).

$$
\begin{aligned}
\textbf{(OPT-R)} \quad & \max && f_{\min} && \\
& \text{s.t.} && g_i^b + h_i^b \le 1 && (i \in \mathcal{N}, b \in \mathcal{B}_i) \\
& && g_i^b \le \textstyle\sum_{l \in \mathcal{L}_{i,b}^{\text{Out}}} z_l^b \le g_i^b A_i && (i \in \mathcal{N}, b \in \mathcal{B}_i) \\
& && h_i^b \le \textstyle\sum_{l \in \mathcal{L}_{i,b}^{\text{In}}} z_l^b \le h_i^b A_i && (i \in \mathcal{N}, b \in \mathcal{B}_i) \\
& && \theta_{ji}^b + \theta_{ij}^b = 1 && (i, j \in \mathcal{N}, b \in \mathcal{B}_{ij}) \\
& && 1 \le \theta_{ik}^b + \theta_{kj}^b + \theta_{ji}^b \le 2 && \\
& && && (\{i,j,k\} \subset \mathcal{N}, b \in \mathcal{B}_i \bigcap \mathcal{B}_j \bigcap \mathcal{B}_k) \\
& && \textstyle\sum_{l \in \mathcal{L}_{i,b}^{\text{Out}}} z_l^b + \sum_{j \in \mathcal{I}_i^b} \lambda_{ji}^b \le A_i g_i^b + (1 - g_i^b) M && (i \in \mathcal{N}, b \in \mathcal{B}_i) \\
& && \lambda_{ji}^b \le \textstyle\sum_{m \in \mathcal{L}_{j,b}^{\text{In}}}^{\text{Tx}(m) \ne i} z_m^b && (i \in \mathcal{N}, b \in \mathcal{B}_i, j \in \mathcal{I}_i^b) \\
& && \lambda_{ji}^b \le A_j \cdot \theta_{ji}^b && (i \in \mathcal{N}, b \in \mathcal{B}_i, j \in \mathcal{I}_i^b) \\
& && \lambda_{ji}^b \ge A_j \cdot \theta_{ji}^b - A_j + \textstyle\sum_{m \in \mathcal{L}_{j,b}^{\text{In}}}^{\text{Tx}(m) \ne i} z_m^b && (i \in \mathcal{N}, b \in \mathcal{B}_i, j \in \mathcal{I}_i^b) \\
& && \textstyle\sum_{l \in \mathcal{L}_{i,b}^{\text{In}}} z_l^b + \sum_{j \in \mathcal{I}_i^b} \mu_{ji}^b \le A_i h_i^b + (1 - h_i^b) M && (i \in \mathcal{N}, b \in \mathcal{B}_i) \\
& && \mu_{ji}^b \le \textstyle\sum_{m \in \mathcal{L}_{j,b}^{\text{Out}}}^{\text{Rx}(m) \ne i} z_m^b && (i \in \mathcal{N}, b \in \mathcal{B}_i, j \in \mathcal{I}_i^b) \\
& && \mu_{ji}^b \le A_j \cdot \theta_{ji}^b && (i \in \mathcal{N}, b \in \mathcal{B}_i, j \in \mathcal{I}_i^b) \\
& && \mu_{ji}^b \ge A_j \cdot \theta_{ji}^b - A_j + \textstyle\sum_{m \in \mathcal{L}_{j,b}^{\text{Out}}}^{\text{Rx}(m) \ne i} z_m^b && (i \in \mathcal{N}, b \in \mathcal{B}_i, j \in \mathcal{I}_i^b) \\
& && f_{\min} \le f(q) && (q \in \mathcal{Q}) \\
& && \textstyle\sum_{q \in \mathcal{Q}}^{l \text{ is traversed by } q} f(q) \le c \cdot \sum_{b \in \mathcal{B}_{\text{Tx}(l),\text{Rx}(l)}} z_l^b && (l \in \mathcal{L}_{\text{Active}}) \\
& && f_{\min}, f(q) \ge 0 && (q \in \mathcal{Q}) \\
& && g_i^b, h_i^b \in \{0,1\} && (i \in \mathcal{N}, b \in \mathcal{B}_i) \\
& && z_l^b \ge 0 && (l \in \mathcal{L}_{\text{Active}}, b \in \mathcal{B}_{\text{Tx}(l),\text{Rx}(l)}) \\
& && \theta_{ji}^b \in \{0,1\} && (i, j \in \mathcal{N}, j \ne i, b \in \mathcal{B}_{ij}) \\
& && \lambda_{ji}^b, \mu_{ji}^b \ge 0 && (i, j \in \mathcal{N}, j \ne i, b \in \mathcal{B}_{ij}) \ .
\end{aligned}
$$

In this formulation, $f_{\min}$, $f(q)$, g_i^b, h_i^b, z_l^b, θ_{ji}^b, λ_{ji}^b, and μ_{ji}^b are optimization variables and A_i, M and c are given constants. The problem is now in the form of Mixed Integer Linear Programming (MILP), which can be solved by CPLEX solver.

3.3.3 Anticipated Results

Before we present numerical results, we offer the following discussion on the possible solution to our problem. Consider a CRN with only a single transmit/receive antenna at each node (i.e., $A_i = 1$, $i \in \mathcal{N}$). Denote f_{CRN} the optimal objective value for this CRN with our problem formulation. Now consider a CRN$^{\text{MIMO}}$ with the same topology as the above CRN, but now with A_{MIMO} transmit/receive antennas at each node. This CRN$^{\text{MIMO}}$ is a special case of our CRN$^{\text{MIMO}}$ network with all $A_i = A_{\text{MIMO}}$, $i \in \mathcal{N}$. Denote $f_{\text{CRN}^{\text{MIMO}}}$ the optimal objective value for this CRN$^{\text{MIMO}}$ under our problem formulation. Comparing $f_{\text{CRN}^{\text{MIMO}}}$ and f_{CRN}, we have the following observation.

Fact 1.

$$f_{CRN^{MIMO}} \geq A_{MIMO} \times f_{CRN} \tag{3.22}$$

The equality part in (3.22) can be easily explained by exploiting spatial multiplexing, i.e., constructing the same solution in CRN$^{\text{MIMO}}$ as that in the CRN but with A_{MIMO} data streams on each link.

However, we are more interested in the possible *inequality* part in (3.22), i.e., with joint channel level (via CR) and co-channel level (via MIMO DoF) optimization within a CRN$^{\text{MIMO}}$, we should anticipate more than A_{MIMO}-fold increase in the optimal solution. The greater the gap is in this inequality, the more potential in the joint CR and MIMO that can be exploited. We shall look into this potential gain via numerical results on various networks in the next section.

3.4 Simulation Results

In this section, we present some numerical results for various network configurations. The goals of this section are two folds. First, we examine how the inter-channel interference and co-channel interference are jointly handled by CR and MIMO DoF, respectively, in an optimal solution for an example network in Section 3.4.2. Then, in Section 3.4.3, we validate the result in Fact 1,

Table 3.2: Network settings

Number of Nodes	Number of Sessions	Network Region
20	4	100×100
30	4	100×100
40	6	100×100
50	8	150×150

particularly the inequality part, thus demonstrating the importance of two-level joint optimization of CR and MIMO.

3.4.1 Simulation Settings

We consider randomly generated CRN$^{\text{MIMO}}$'s with $|\mathcal{N}|$ = 20, 30, 40 and 50 nodes. For ease of scalability and generality, we normalize all units for distance, bandwidth, and rate with appropriate dimensions. The number of sessions and network region for each network configuration are shown in Table 3.2. All nodes are randomly located within their network region. For each network configuration, the source node and destination node for each session are randomly selected. There are $|\mathcal{B}| = 15$ frequency bands available in the network. The set of available bands at each node is randomly selected from the 15-band pool. The capacity achieved by one band and one DoF is normalized to 1. We assume that the transmission range is 30 and the interference range is 60.

3.4.2 Results for A 30-Node Network

Before we present complete results for all four network configurations, we select one network configuration and explain the details of its optimal solution. This will offer us thorough understanding when we present results for the other network configurations.

The particular network configuration that we will examine is the 30-node CRN$^{\text{MIMO}}$ shown

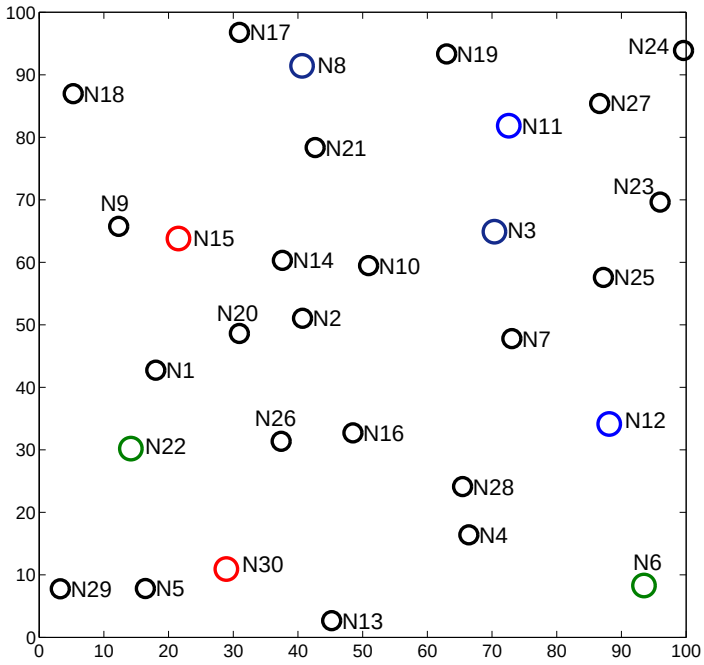

(a) Topology for the 30-node CRN^{MIMO}.

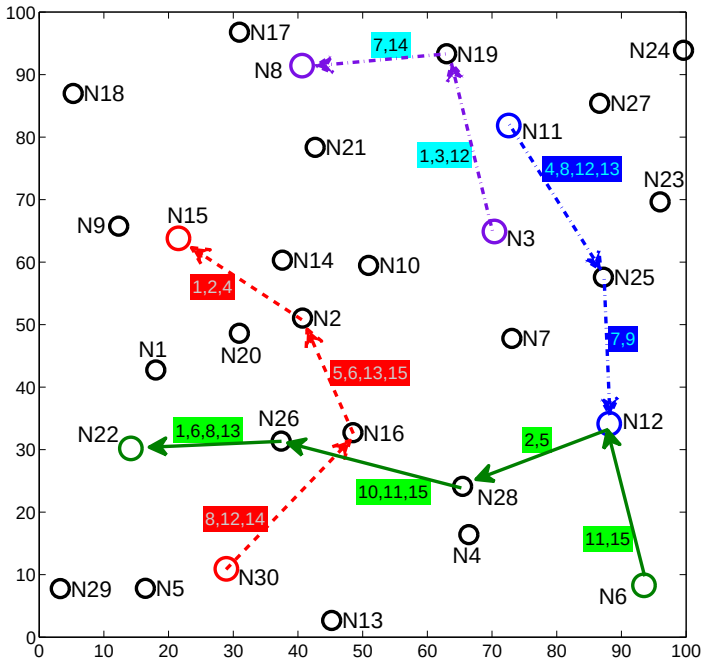

(b) Solution for the 30-node CRN^{MIMO}.

Figure 3.4: A 30-node CRN^{MIMO}.

Table 3.3: Each node's location and available frequency bands for the 30-node CRN$^{\text{MIMO}}$

Node	Location	Available Bands	Node	Location	Available Bands
N1	(18.0, 42.7)	1,2,4,5,6,8,9,10,11,12,13,14	N16	(48.5, 32.7)	2,4,5,6,8,10,11,12,13,14,15
N2	(40.7, 51.0)	1,2,4,5,6,7,8,9,10,11,13,14,15	N17	(31.0, 96.8)	4,6,7,12,15
N3	(70.4, 64.9)	1,2,3,4,5,7,8,9,12,13,14,15	N18	(5.3 , 87.0)	6,7,15
N4	(66.4, 16.4)	2,7,10	N19	(63.0, 93.3)	1,3,4,7,12,14
N5	(16.4, 7.8)	5,6,9,10,12,13,14	N20	(30.9, 48.6)	1,2,4,6,8,9,10,11,12,13,14
N6	(93.5, 8.3)	11,15	N21	(42.7, 78.4)	1,3,4,7,12,14
N7	(73.1, 47.8)	1,2,3,4,5,7,8,9,13,15	N22	(14.2, 30.2)	1,2,5,6,8,9,10,11,12,13,14
N8	(40.6, 91.4)	4,6,7,12,14	N23	(99.0, 69.6)	1,2,3,4,7,9,12,13,15
N9	(12.3, 65.8)	1,2,7,14	N24	(99.6, 93.9)	3,9,12
N10	(50.9, 59.5)	1,2,3,4,5,6,7,8,11,14,15	N25	(87.2, 57.6)	1,2,4,5,7,8,9,12,13,15
N11	(72.6, 81.9)	1,2,3,4,5,7,8,9,12,13,14,15	N26	(37.4, 31.4)	1,2,4,5,6,8,9,10,11,12,13,14,15
N12	(88.1, 34.1)	2,5,7,9,11,15	N27	(86.6, 85.4)	1,2,3,4,7,9,12,13
N13	(45.2, 2.7)	10,12,13,14	N28	(65.5, 24.1)	2,5,7,10,11,15
N14	(37.6, 60.3)	1,2,4,5,6,7,8,10,11,13,14,15	N29	(3.3 , 7.8)	5,6,9,13
N15	(21.5, 63.8)	1,2,4,7,8,10,14	N30	(28.9, 10.9)	5,6,8,9,10,11,12,13,14

Table 3.4: Source and destination nodes of each session in the 30-node CRN$^{\text{MIMO}}$

Session q	Source Node $s(q)$	Destination Node $d(q)$
1	N30	N15
2	N6	N22
3	N11	N12
4	N3	N8

in Fig. 3.4(a). The location and available bands for each node are listed in Table 3.3. Table 3.4 specifies the source and destination nodes for each session. For MIMO, we assume each node in the network is equipped with four antennas. We assume minimum-hop routing is used in the network.

Using CPLEX, we can obtain an optimal solution to the OPT-R problem. The optimal objective value for this 30-node CRN$^{\text{MIMO}}$ is 6, which means each session can send at least 6 data streams from its source to its destination.

In addition to the optimal objective value, we show channel level and co-channel level solution to achieve this objective. Figure 3.4(b) shows the optimal band assignment on each link for each session. The bands assigned on each link are shown in shaded boxes. This result is also shown in Table 3.5 (first 3 columns). Also shown in column 4 of Table 3.5 is the capacity on each band under the optimal solution. In column 5, we show the capacity (in terms of sum of capacity on each band) over each link. Note that this capacity is at least 6, thus guaranteeing each session can transport at least 6 data streams.

We now examine co-channel DoF allocation in the optimal solution. Recall that DoF allocation is performed within the same band. Given that we have a total of 15 bands in the network, we shall have DoF allocation within each of the 15 bands. Let's first show DoF allocation in one particular band, say band 1. Note that band 1 is used by links N2 $\rightarrow$ N15, N3 $\rightarrow$ N19, N26 $\rightarrow$ N22 in Fig. 3.4(b). The DoF allocation on these 6 nodes are given in Fig. 3.5 and Table 3.6. As shown in Fig. 3.5, there are 2 data streams on each of these 3 links on band 1. The dashed lines in Fig. 3.5 shows the interference relationship among the nodes, i.e., node N2 interferes N19 and N22, node N3 interferes N15, and node N26 interferes N15. These transmission links and interference relationships are also listed in Table 3.6 (row 1), where "N2 $\rightarrow$ N15 (N19, N22)" denotes N2 transmits to N15 and interferes N19 and N22, etc. Also shown in the first column of Table 3.6 is the optimal order for the 6 nodes for DoF allocation in the optimal solution, i.e., N2, N3, N15, N19, N26, N22. Based on this order, the DoFs at each node are allocated as follows (also see Fig. 3.5).

Table 3.5: Details of band assignment, capacity on each band, and capacity on each link in the 30-node CRN$^{\text{MIMO}}$

Session q	Link	Assigned Band	Capacity on Band	Link Capacity
1	N30 → N16	8	1	6
		12	1	
		14	4	
	N16 → N2	5	1	6
		6	3	
		13	1	
		15	1	
	N2 → N15	1	2	6
		2	1	
		4	3	
2	N6 → N12	11	3	6
		15	3	
	N12 → N28	2	3	6
		5	3	
	N28 → N26	10	4	6
		11	1	
		15	1	
	N26 → N22	1	2	7
		6	1	
		8	1	
		13	3	
3	N11 → N25	4	1	6
		8	2	
		12	2	
		13	1	
	N25 → N12	7	2	6
		9	4	

Table 3.5: Details of band assignment, capacity on each band, and capacity on each link in the 30-node CRN^{MIMO} (continued)

Session q	Link	Assigned Band	Capacity on Band	Link Capacity
4	N3 → N19	1	2	7
		3	4	
		12	1	
	N19 → N8	7	2	6
		14	4	

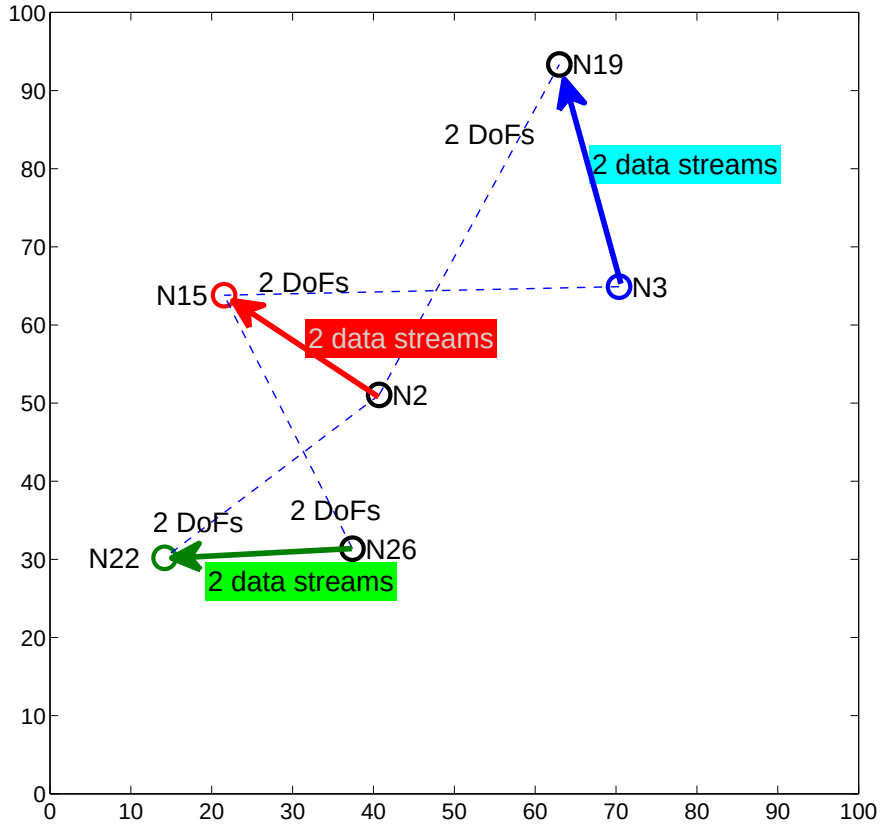

Figure 3.5: The DoF allocation in the optimal solution on band 1 for the 30-node CRN^{MIMO}.

Table 3.6: The DoFs allocation on band 1 in the 30-node CRN^{MIMO}

Transmission and Interference	N2 → N15 (N19, N22), N3 → N19 (N15), N26 → N22 (N15)	
Ordered Node List	Interference Cancellation (# of DoFs, To/From, Node)	Spatial Multiplexing (# of DoFs, Transmit/Receive, Node)
N2		(2, Transmit, N15)
N3		(2, Transmit, N19)
N15	(2, From, N3)	(2, Receive, N2)
N19	(2, From, N2)	(2, Receive, N3)
N26	(2, To, N15)	(2, Transmit, N22)
N22	(2, To, N2)	(2, Receive, N26)

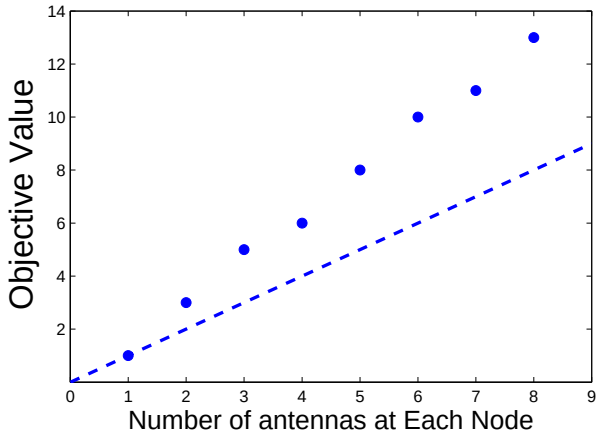

Figure 3.6: Objective value under different antennas for the 30-node CRN^{MIMO}.

Table 3.7: The DoFs allocation on band 2–15 in the example 30-node CRN$^{\text{MIMO}}$

Band 2		
Transmission and Interference	N2 → N15 (N28), N12 → N28	
Ordered Node List	Interference Cancellation	Spatial Multiplexing
N15		(1, Receive, N2)
N28		(3, Receive, N12)
N2	(3, To, N28)	(1, Transmit, N15)
N12		(3, Transmit, N28)
Band 3		
Transmission and Interference	N3 → N19	
Ordered Node List	Interference Cancellation	Spatial Multiplexing
N3		(4, Transmit, N19)
N19		(4, Receive, N3)
Band 4		
Transmission and Interference	N2 → N15 (N25), N11 → N25 (N15)	
Ordered Node List	Interference Cancellation	Spatial Multiplexing
N25		(1, Receive, N11)
N2	(1, To, N25)	(3, Transmit, N15)
N11		(1, Transmit, N25)
N15	(1, From, N11)	(3, Receive, N2)
Band 5		
Transmission and Interference	N12 → N28 (N2), N16 → N2 (N28)	
Ordered Node List	Interference Cancellation	Spatial Multiplexing
N16		(1, Transmit, N2)
N28	(1, From, N16)	(3, Receive, N12)
N2		(1, Receive, N16)
N12	(1, To, N2)	(3, Transmit, N28)
Band 6		
Transmission and Interference	N16 → N2 (N22), N26 → N22 (N2)	
Ordered Node List	Interference Cancellation	Spatial Multiplexing
N2		(3, Receive, N16)
N26	(3, To, N2)	(1, Transmit, N22)
N16		(3, Transmit, N2)
N22	(3, From, N16)	(1, Receive, N26)

Table 3.7: The DoFs allocation on band 2–15 in the example 30-node CRN^{MIMO} (continued)

Band 7		
Transmission and Interference	N19 → N8, N25 → N12 (N8)	
Ordered Node List	Interference Cancellation	Spatial Multiplexing
N8		(2, Receive, N19)
N12		(2, Receive, N25)
N19		(2, Transmit, N8)
N25	(2, To, N8)	(2, Transmit, N12)

Band 8		
Transmission and Interference	N11 → N25 (N16), N26 → N22 (N16, N25), N30 → N16 (N22)	
Ordered Node List	Interference Cancellation	Spatial Multiplexing
N25		(2, Receive, N11)
N26	(2, To, N25)	(1, Transmit, N22)
N30		(1, Transmit, N16)
N11		(2, Transmit, N25)
N22	(1, From, N30)	(1, Receive, N26)
N16	(1, From, N26) (2, From, N11)	(1, Receive, N30)

Band 9		
Transmission and Interference	N25 → N12	
Ordered Node List	Interference Cancellation	Spatial Multiplexing
N12		(4, Receive, N25)
N25		(4, Transmit, N12)

Band 10		
Transmission and Interference	N28 → N26	
Ordered Node List	Interference Cancellation	Spatial Multiplexing
N26		(4, Receive, N28)
N28		(4, Transmit, N26)

Band 11		
Transmission and Interference	N6 → N12, N28 → N26 (N12)	
Ordered Node List	Interference Cancellation	Spatial Multiplexing
N6		(3, Transmit, N12)
N12		(3, Receive, N6)
N28	(3, To, N12)	(1, Transmit, N26)
N26		(1, Receive, N28)

Table 3.7: The DoFs allocation on band 2–15 in the example 30-node CRN^{MIMO} (continued)

Band 12		
Transmission and Interference	N3 → N19 (N16, N25), N11 → N25 (N16, N19), N30 → N16	
Ordered Node List	Interference Cancellation	Spatial Multiplexing
N30		(1, Transmit, N16)
N11		(2, Transmit, N25)
N16	(2, From, N11)	(1, Receive, N30)
N25		(2, Receive, N11)
N3	(1, To, N16) (2, To, N25)	(1, Transmit, N19)
N19	(2, From, N11)	(1, Receive, N3)

Band 13		
Transmission and Interference	N11 → N25 (N2), N16 → N2 (N22, N25), N26 → N22 (N2, N25)	
Ordered Node List	Interference Cancellation	Spatial Multiplexing
N2		(1, Receive, N16)
N26	(1, To, N2)	(3, Transmit, N22)
N25	(3, From, N26)	(1, Receive, N11)
N16	(1, To, N25)	(1, Transmit, N2)
N22	(1, From, N16)	(3, Receive, N26)
N11	(1, To, N2)	(1, Transmit, N25)

Band 14		
Transmission and Interference	N19 → N8, N30 → N16	
Ordered Node List	Interference Cancellation	Spatial Multiplexing
N30		(4, Transmit, N16)
N8		(4, Receive, N19)
N16		(4, Receive, N30)
N19		(4, Transmit, N8)

Band 15		
Transmission and Interference	N6 → N12, N16 → N2 (N12, N26), N28 → N26 (N2, N12)	
Ordered Node List	Interference Cancellation	Spatial Multiplexing
N2		(1, Receive, N16)
N6		(3, Transmit, N12)
N28	(1, To, N2)	(1, Transmit, N26)
N12	(1, From, N28)	(3, Receive, N6)
N16	(3, To, N12)	(1, Transmit, N2)
N26	(1, From, N16)	(1, Receive, N28)

- Starting with node N2, it is the first node in the ordered node list and it is a transmitting node. Then it allocates 2 DoFs to transmit 2 data streams to node N15. It does not need to allocate any DoF to cancel potential interference to other receiving nodes after itself in the node list, i.e., node N19 and N22.

- The next node in the list is N3. As a transmitting node, it allocates 2 DoFs for transmitting 2 data streams to node N19. It does not need to allocate any DoF to cancel potential interference to receiving node N15, which is after itself in the ordered node list.

- The next node in the list is N15. As a receiving node, it needs to allocate 2 DoFs for receiving 2 data streams from node N2. In addition, it must ensure that its reception is not interfered by any transmitting node before itself in the list, i.e., N3. Thus it allocates the remaining 2 DoFs to cancel the interference from node N3.

- The next node in the list is N19. As a receiving node, it allocates 2 DoFs for receiving 2 data streams from node N3. In addition, it allocates the remaining 2 DoFs to cancel interference from transmitting node N2 which is before itself in the list.

- The next node in the list is N26. As a transmitting node, it needs to ensure that its transmission does not interfere with any receiving node before itself in the list, i.e., N15. For this purpose, it allocates 2 DoFs to cancel its interference to node N15. Then it allocates the remaining 2 DoFs to transmit 2 data streams to node N22.

- The last node in the list is N22. As a receiving node, it allocates 2 DoFs to receiving 2 data streams from node N22. In addition, it must ensure that its reception is not interfered by any transmitting node before itself in the list, i.e., N2. Thus, it allocates the remaining 2 DoFs to cancel the interference from node N2.

This completes the DoF allocation for each node in the list on band 1. The DoF allocation for the 6 nodes is also listed in Table 3.6, where we employ the following two abbreviated notations.

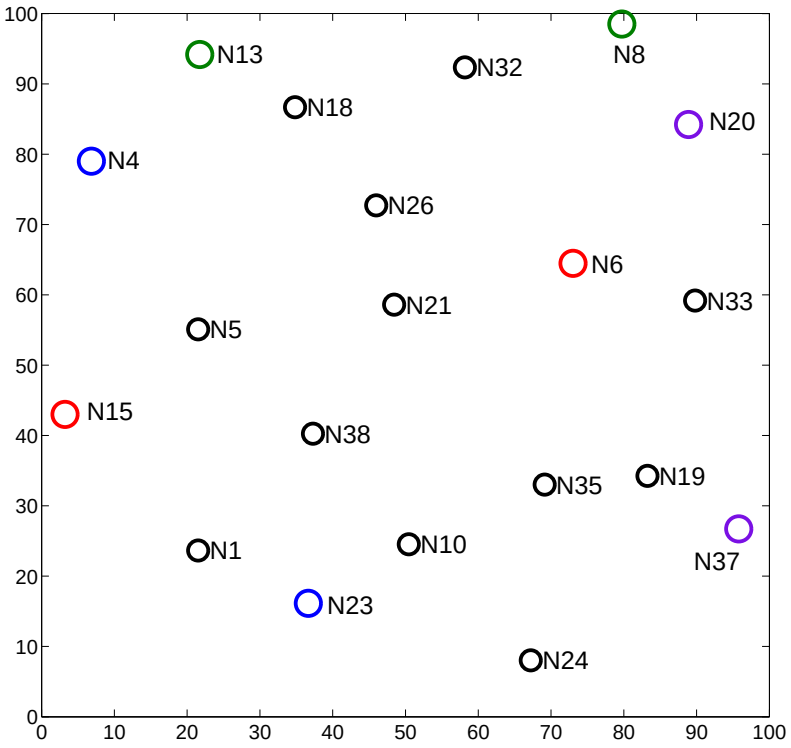

(a) Topology for a 20-node CRN^{MIMO}.

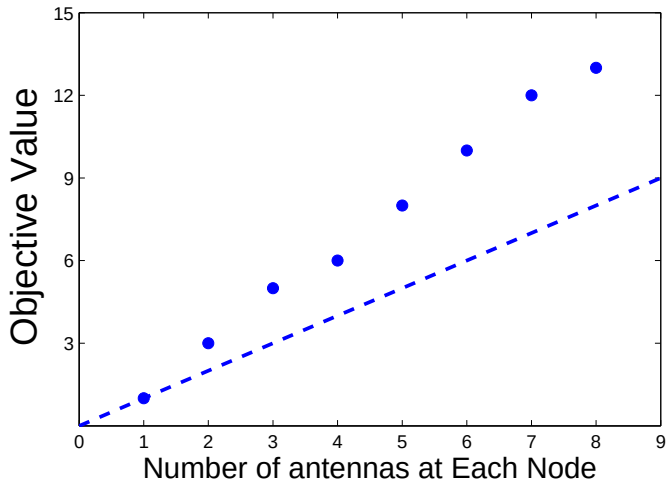

(b) Objective value under different antennas for a 20-node CRN^{MIMO}.

Figure 3.7: Comparison of $f_{\text{CRN}^{\text{MIMO}}}$ vs $A_{\text{MIMO}} \times f_{\text{CRN}}$ for a 20-node network.

Table 3.8: Each node's location and available frequency bands for a 20-node CRN$^{\text{MIMO}}$

Node	Location	Available Bands	Node	Location	Available Bands
N1	(21.5, 23.6)	6,7,8,11,12,13,14,15	N11	(48.4, 58.6)	1,3,5,7,8,11,13,15
N2	(6.8, 79.0)	3,8,14	N12	(36.7, 16.1)	6,7,8,9,11,12,13,14
N3	(21.5, 55.1)	1,3,5,7,8,12,13,14,15	N13	(67.2, 8.0)	6,9,11,12,15
N4	(73.0, 64.5)	1,3,5,7,8	N14	(46.0, 72.7)	1,2,3,4,5,8,10,11,13,14,15
N5	(79.7, 98.5)	1,2,3,4,8,9,10	N15	(58.2, 92.4)	1,2,3,4,5,8,10,11,15
N6	(50.5, 24.5)	6,7,8,9,11,12,13,15	N16	(89.8, 59.2)	1,5,7,8,10,12
N7	(21.7, 94.2)	2,3,11,14	N17	(69.1, 33.0)	6,7,8,9,12,15
N8	(3.2, 43.0)	3,7,8,13,14,15	N18	(95.8, 26.7)	4,10,15
N9	(34.8, 86.7)	2,3,4,5,10,11,14,15	N19	(37.3, 40.3)	1,3,5,6,7,8,12,13,14,15
N10	(83.2, 34.3)	4,6,7,10,15	N20	(88.9, 84.2)	1,2,3,5,8,9,10,12

Table 3.9: Source and destination nodes of each session in a 20-node CRN$^{\text{MIMO}}$

Session q	Source Node $s(q)$	Destination Node $d(q)$
1	N4	N8
2	N7	N5
3	N12	N2
4	N18	N20

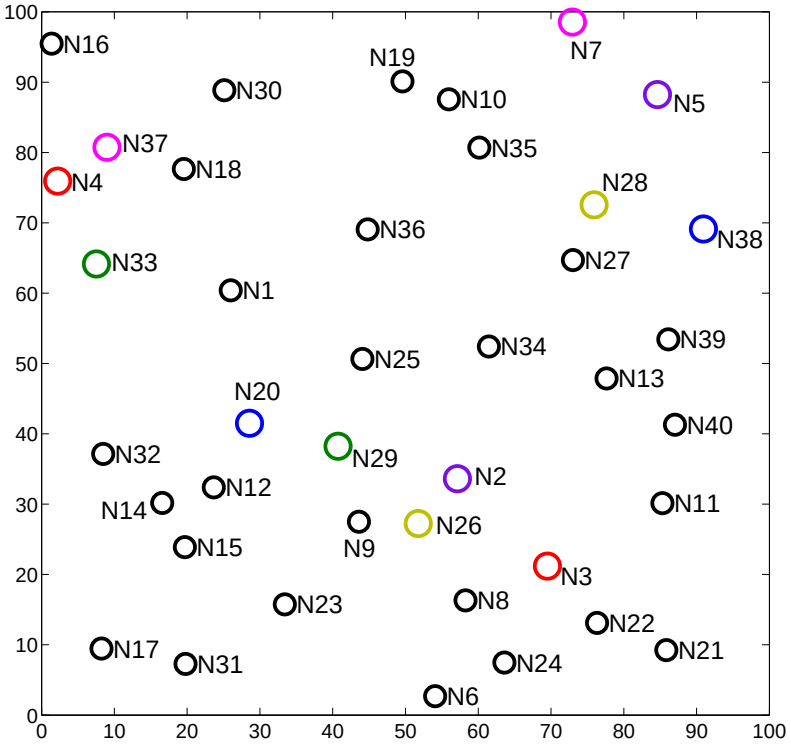

(a) Topology for a 40-node CRN$^{\text{MIMO}}$.

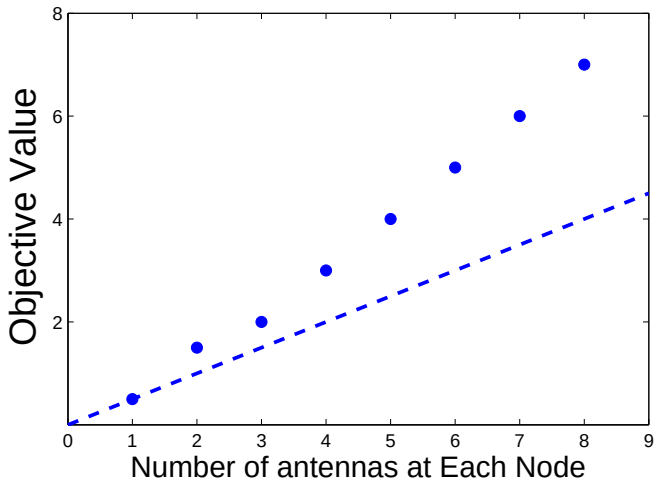

(b) Objective value under different antennas for a 40-node CRN$^{\text{MIMO}}$.

Figure 3.8: Comparison of $f_{\text{CRN}^{\text{MIMO}}}$ vs $A_{\text{MIMO}} \times f_{\text{CRN}}$ for a 40-node network.

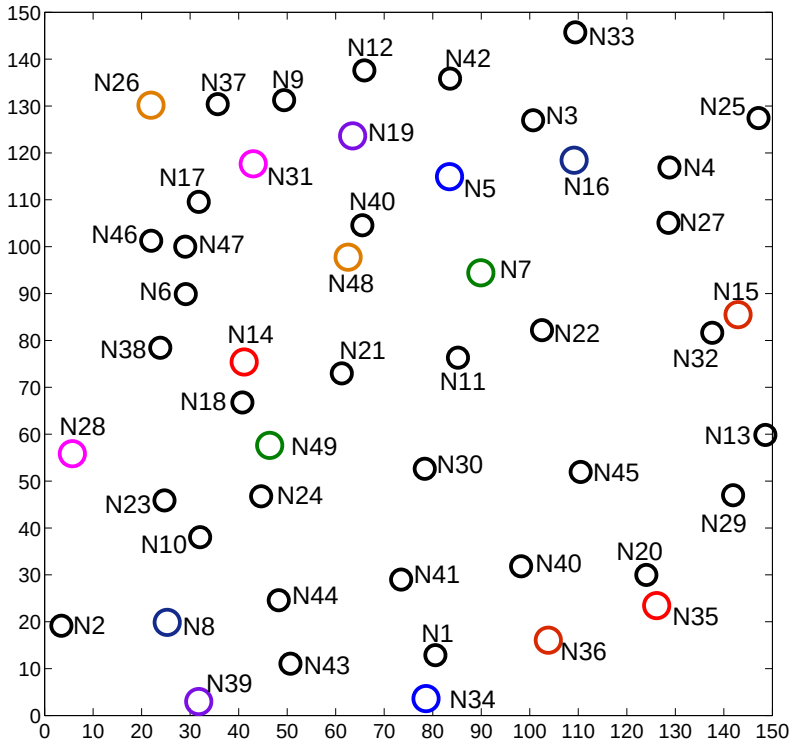

(a) Topology for a 50-node CRN$^{\text{MIMO}}$.

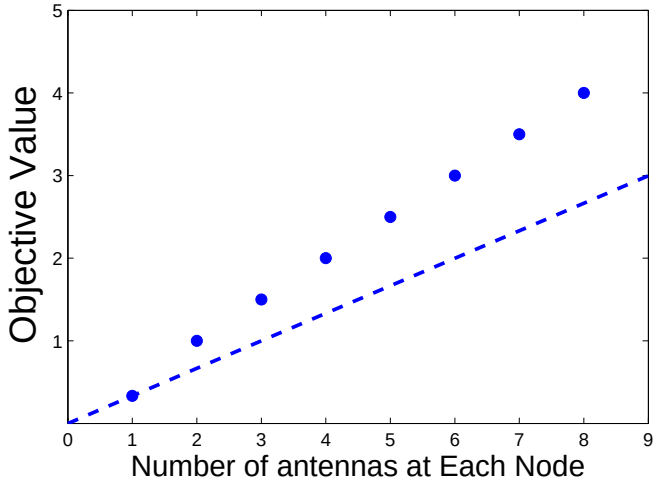

(b) Objective value under different antennas for a 50-node CRN$^{\text{MIMO}}$.

Figure 3.9: Comparison of $f_{\text{CRN}^{\text{MIMO}}}$ vs $A_{\text{MIMO}} \times f_{\text{CRN}}$ for a 50-node network.

Table 3.10: Each node's location and available frequency bands for a 40-node CRN^{MIMO}

Node	Location	Available Bands	Node	Location	Available Bands
N1	(26.0, 60.4)	1,2,4,6,7,8,10,11,12,13,15	N21	(85.8, 9.2)	3,5,6,8,9,14,15
N2	(57.1, 33.6)	2,3,5,7,8,13	N22	(76.3, 13.1)	2,3,5,6,8,9,14,15
N3	(69.5, 21.2)	2,3,5,6,8,9,13,14	N23	(33.4, 15.7)	10,11,13,14
N4	(2.2 , 75.9)	2,4,8,13,15	N24	(63.6, 7.4)	3,5,6,8
N5	(84.6, 88.2)	1,3,5,9,10,11,12	N25	(44.1, 50.6)	1,2,7,8,10,11,12,13,15
N6	(54.1, 2.7)	3,9	N26	(51.8, 27.2)	2,3,8,10,13
N7	(72.9, 98.5)	1,2,3,5,9,10,11	N27	(73.0, 64.7)	3,7,12,13,15
N8	(58.3, 16.3)	2,3,5,6,8,13	N28	(75.9, 72.6)	1,3,5,7,10,11,12,15
N9	(43.6, 27.5)	2,3,10,13	N29	(40.7, 38.2)	1,2,7,10,11,12,13
N10	(56.0, 87.6)	1,2,3,6,8,9,10,12,15	N30	(25.1, 88.9)	1,2,4,6,7,8,10,12,13,15
N11	(85.3, 30.1)	2,5,6,7,8,9,11,13,14,15	N31	(19.8, 7.2)	10,14
N12	(23.7, 32.4)	4,10,11,13,14	N32	(8.5 , 37.1)	4,10,11,13,14
N13	(77.6, 47.9)	2,5,7,8,9,11,12,13	N33	(7.5 , 64.2)	1,2,4,7,8,11,13
N14	(16.6, 30.1)	4,10,11,13,14	N34	(61.5, 52.4)	2,3,7,12,13,15
N15	(19.7, 23.9)	10,11,14	N35	(60.1, 80.7)	1,2,3,6,7,8,9,10,12,15
N16	(1.4 , 95.5)	4,15	N36	(44.8, 69.1)	1,2,3,4,6,7,8,10,12,13,15
N17	(8.2 , 9.5)	10,14	N37	(9.0 , 80.7)	1,2,4,7,8,13,15
N18	(19.5, 77.7)	1,2,4,6,7,8,12,13,15	N38	(90.9, 69.1)	3,5,7,11,12
N19	(49.6, 90.1)	2,3,6,8,9,10,12,15	N39	(86.1, 53.4)	7,9,11,12,13
N20	(28.6, 41.5)	1,4,7,10,11,12,13,14	N40	(87.0, 41.3)	2,5,6,7,8,9,11,12,13,15

Table 3.11: Source and destination nodes of each session in a 40-node CRN$^{\text{MIMO}}$

Session q	Source Node $s(q)$	Destination Node $d(q)$
1	N3	N4
2	N29	N33
3	N38	N20
4	N5	N2
5	N7	N37
6	N28	N26

- We use the tuple (# of DoFs, From/To, Node) to denote the interference cancellation relationship between nodes. For example, (2, From, N3) denotes current node (in the first column of the same row) allocates 2 DoFs to cancel the interference from N3, whereas (2, To, N15) denotes current node allocates 2 DoFs to cancel its interference to N15.
- We use the tuple (# of DoFs, Transmit/Receive, Node) to denote data transmission relationship between the nodes. For example, (2, Transmit, N15) denotes the current node (in the first column of the same row) allocates 2 DoFs to transmit data streams to N15, whereas (2, Receive, N2) denotes the current node uses 2 DoFs to receive data streams from N2.

Given the above explanation of DoF allocation on band 1, we now present DoF allocations on bands 2 to 15, which are listed in Table 3.7.

3.4.3 $f_{\text{CRN}^{\text{MIMO}}}$ vs. $A_{\text{MIMO}} \times f_{\text{CRN}}$

The results in the last section give details in an optimal solution for a 30-node CRN$^{\text{MIMO}}$ with $A_{\text{MIMO}} = 4$ antennas at each node. We now validate the result in (3.22) under different number of antennas at each node. Figure 3.6 shows the optimal objective values under different number of antennas for the same 30-node network discussed in the last section. Also shown in this figure is a

Table 3.12: Each node's location and available frequency bands for a 50-node CRN^{MIMO}

Node	Location	Available Bands	Node	Location	Available Bands
N1	(80.5, 12.9)	1,9	N26	(21.9, 130.2)	4,8,10,14
N2	(3.5, 19.1)	11,15	N27	(128.6, 105.1)	2,4,5,6,7,8,14
N3	(100.7, 127.0)	2,5,6,8,12,13,14	N28	(5.7, 55.9)	10,11,12,15
N4	(128.8, 116.9)	2,4,5,6,7,8,12,14	N29	(141.9, 47.0)	1,2,3,7,10,13
N5	(83.5, 114.9)	2,3,5,8,11,12,13,14,15	N30	(78.3, 52.6)	1,3,4,5,6,13,15
N6	(29.1, 89.9)	3,4,9,10,11,12,14	N31	(43.0, 117.7)	3,4,8,9,10,11,12,13,14
N7	(89.9, 94.4)	2,3,4,5,6,11,13,14,15	N32	(137.6, 81.6)	2,4,5,6,7,10,13
N8	(25.3, 19.9)	11,15	N33	(109.4, 145.7)	2,5,6,8,12,13,14
N9	(49.4, 131.2)	3,4,5,8,9,10,11,12,13,14	N34	(78.6, 3.6)	1,9
N10	(32.0, 38.0)	1,11,15	N35	(126.2, 23.4)	1,3,9,10,13
N11	(85.2, 76.3)	1,2,3,4,5,6,11,13,15	N36	(103.8, 16.1)	1,3,9,13
N12	(65.9, 137.6)	5,8,12,13,14	N37	(35.7, 130.4)	3,4,8,9,10,13,14
N13	(148.6, 59.8)	2,3,4,7,10,13	N38	(23.8, 78.4)	3,4,9,10,11,12,15
N14	(41.1, 75.4)	3,4,5,9,10,11,12,15	N39	(31.8, 3.0)	11,15
N15	(142.9, 85.5)	2,4,5,6,7,10	N40	(98.2, 31.8)	1,3,4,6,9,13,15
N16	(109.1, 118.4)	2,4,5,6,7,8,12,13,14	N41	(73.5, 29.0)	1,3,9,11,13,15
N17	(31.8, 109.6)	3,4,8,9,10,11,12,14	N42	(83.6, 135.9)	2,5,8,12,13,14
N18	(40.8, 66.8)	3,4,5,9,10,11,12,15	N43	(50.7, 11.1)	1,11,15
N19	(63.5, 123.6)	3,4,5,8,9,10,11,12,13,14	N44	(48.3, 24.6)	1,11,15
N20	(124.0, 30.0)	1,3,4,9,10,13	N45	(110.5, 51.9)	1,3,4,6,9,13,15
N21	(61.2, 73.0)	3,4,5,6,9,10,11,12,13,15	N46	(22.0, 101.3)	3,4,8,9,10,11,12,14
N22	(102.5, 82.2)	1,2,3,4,5,6,13,14,15	N47	(29.0, 100.0)	3,4,8,9,10,11,12,14
N23	(24.7, 45.9)	10,11,12,15	N48	(62.6, 97.8)	3,4,5,9,10,11,12,13,14,15
N24	(44.6, 46.8)	1,3,5,10,11,12,15	N49	(46.4, 57.6)	1,3,5,10,11,12,15
N25	(147.1, 127.4)	2,4,5,6,7,8	N50	(65.5, 104.6)	3,4,5,8,9,10,11,12,13,14,15

Table 3.13: Source and destination nodes of each session in a 50-node CRN$^{\text{MIMO}}$

Session q	Source Node $s(q)$	Destination Node $d(q)$
1	N35	N14
2	N8	N16
3	N34	N5
4	N39	N19
5	N31	N28
6	N36	N15
7	N49	N7
8	N26	N48

dashed line with a slope of f_{CRN}. Note that the equality in (3.22) only coincides for the first point, i.e., single antenna at each node. When the number of antennas at each node is greater than 1, we have an inequality, i.e., $f_{\text{CRN}^{\text{MIMO}}} > A_{\text{MIMO}} \times f_{\text{CRN}}$. That is, with joint channel level (via CR) and co-channel level (via MIMO DoF) optimization within a CRN$^{\text{MIMO}}$ network, we have more than A_{MIMO}-fold increase in the optimal solution. This confirms that joint optimization of CR at channel level and MIMO at co-channel level for interference mitigation is necessary.

In Figs. 3.7, 3.8, and 3.9, we further compare $f_{\text{CRN}^{\text{MIMO}}}$ vs. $A_{\text{MIMO}} \times f_{\text{CRN}}$ for 20-, 40-, 50-node networks under varying number of antennas, respectively. The location and available bands at each node and source/destination node of each session are given in Tables 3.8 to 3.13 for the three networks. Again, we confirm our findings that joint optimization of CR at channel level and MIMO at co-channel level offers more capacity than A_{MIMO}-fold increase in capacity in a CRN.

3.5 Conclusion

In this chapter, we explored joint optimization of CR and MIMO in a multi-hop ad hoc network. By exploiting CR's behavior at channel level and MIMO's capability within a channel, we showed

that we can have much bigger design space to mitigate interference in the network. We developed a tractable mathematical model for a CRN^{MIMO} that captures the essence of channel assignment (for CR) and DoF allocation (for MIMO). Based on this mathematical model, we used numerical results to show how channel assignment in CRN and DoF allocation in MIMO can be jointly optimized to maximize capacity. More important, for a CRN^{MIMO} with A_{MIMO} antennas at each node, we showed that the joint optimization of CR and MIMO offers more than A_{MIMO}-fold capacity increase than a CRN with only a single antenna at each node.

Chapter 4

Summary and Future Work

4.1 Summary of Contributions

In recent years, CR has quickly been accepted as the enabling radio technology for next-generation wireless communications. With unique characteristics associated with CR, new models and theoretical results, along with new mathematical techniques, need to be developed. In this thesis, we studied the important problem associated with CR ad hoc networks. The main contributions of this thesis are the following.

1. We studied the multicast communications in CRNs. We showed how to minimize the required network resource to support a set of multicast sessions, each associated with a given flow rate. Following a cross-layer approach, with joint consideration of frequency band scheduling and multicast routing, we formulated the resource optimization problem into a mixed integer linear program (MILP). Then we developed a polynomial time algorithm that incorporates several novel ideas such as identification of key integer variables, fixing these variables via a series of relaxed linear programming, and tying up such integer fixing with a bottom-up tree construction. Based on simulation results, we showed that the solutions obtained by our proposed algorithm are highly competitive.

2. We studied the capacity problem of joint optimization of MIMO and CRN. We showed that we can have much bigger design space to mitigate interference in the network, by exploiting CR's behavior at channel level and MIMO's capability within a channel. We developed a tractable mathematical model for a CRN$^{\text{MIMO}}$. The mathematical model captures the essence of channel assignment and DoF allocation. This joint optimization problem was formulated into a mathematical program with the goal of maximizing the minimum rate among user sessions. Using the numerical results obtained by the mathematical model, we showed how channel assignment in CRN and DoF allocation in MIMO can be jointly optimized to maximize capacity. More important, we showed that with joint optimization of CR and MIMO (CRN$^{\text{MIMO}}$), the network capacity gains more than A_{MIMO}-fold increase comparing to the CRN with only a single antenna at each node.

4.2 Future Research Directions

The following problems remain open and will be my future research.

- For the multicast problem under CRN, we presented an efficient algorithm which offers highly competitive solution. Although we showed that our solution is near-optimal, it remains a heuristic solution. In our future work, we will consider developing a provably optimal solution.

- For the CRN$^{\text{MIMO}}$, we showed that it is necessary to consider joint optimization of CR at channel level and MIMO at co-channel level for interference mitigation. In our future work, we will offer a more formal (theoretical) study on this problem. We want to explore when the capacity gain will be strictly greater than A_{MIMO}-fold increase. We will analyze the gap between the two based on theoretical results.

- In this thesis, our study of CRN is based on the so-called "protocol model". Another interference model is the so-called "physical model", which is considered to be a more accurate, but

also more complex interference model. The interference relationship in physical model is computed via signal to interference plus noise ratio (SINR) directly. This model introduces non-linear term in the formulation and is more difficult to analyze. In our future work, we will consider how to use this interference model for joint optimization of MIMO and CR.

Bibliography

[1] M. Alicherry, R. Bhatia, and L. Li, "Joint channel assignment and routing for throughput optimization in multi-radio wireless mess networks", *in Proc. ACM Mobicom,* pp. 58–72, Cologne, Germany, Aug.–Sept. 2005.

[2] R. Bhatia and L. Li, "Characterizing achievable multicast rates in multi-hop wireless networks," *in Proc. ACM Mobihoc,* pp. 133–144, Urbana-Champaign, IL, May 2005.

[3] R. Bhatia and L. Li, "Throughput optimization of wireless mesh networks with MIMO links," *in Proc. IEEE Infocom,* pp. 2326–2330, Anchorage, AK, May 2007.

[4] E. Biglieri, R. Calderbank, A. Constantinides, A. Goldsmith, A. Paulraj, and H.V. Poor, *MIMO Wireless Communications,* Cambridge University Press, Jan. 2007.

[5] G. Caire and S. Shamai, "On the achievable throughput of a multiantenna gaussian broadcast channel," *IEEE Trans. on Information Theory,* vol. 49, no. 7, pp. 1691–1706, July 2003.

[6] M.X. Cheng, J. Sun, M. Min, Y. Li, W. Wu, "Energy-efficient broadcast and multicat routing in multihop ad hoc wireless networks," *in Proc. ACM Wireless Comm. & Mobile Compu.,* vol. 6, no. 2, pp. 213–223, March, 2006.

[7] S. Chu and X. Wang, "Opportunistic and cooperative spatial multiplexing in MIMO ad hoc networks," *in Proc. ACM Mobihoc,* pp. 63–72, Hong Kong, China, May 2008.

[8] A.K. Das, R.J. Marks, M. El-Sharkawi, P. Arabshahi, and A. Gray, "Minimum power broadcast trees for wireless networks: Integer programming formulations," *in Proc. IEEE Infocom,* vol. 2, pp. 1001–1010, San Francisco, CA, March–April 2003.

[9] G.J. Foschini, "Layered space-time architecture for wireless communication in a fading envorinment when using multi-element antennas," *Bell Labs Tech. J.,* vol. 1, no. 2, pp. 41–59, 1996.

[10] M.R. Garey and D.S. Johnson, *Computers and Intractability: A Guide to the Theory of NP-completenes, W.H. Freeman and Company,* pp. 245–248, New York, NY, 1979.

[11] S. Guo, M. Guo, and V. Leung, "Exploring the multicast lifetime capacity of WANETs with directional multibeam antennas," *in Proc. IEEE Infocom*, Rio de Janeiro, Brazil, April 2009.

[12] S. Guo, O. Yang, "Antenna orientation optimization for minimum-energy multicast tree construction in wireless ad hoc networks with directional antennas," *in Proc. ACM Mobihoc*, pp. 234–243, Tokyo, Japan, May 2004.

[13] S. Guo, O. Yang, V. Leung, "Approximation algorithms for longest-lived directional multicast communications in WANETs," *in Proc. ACM Mobihoc*, pp. 190–198, Montreal, Quebec, Canada, Sept. 2007.

[14] D. Gesbert, M. Shafi, D.S. Shiu, P.J. Smith, and A. Naguib, "From theory to practice: An overview of MIMO space-time coded wireless systems," *IEEE J. Sel. Areas Commun.*, vol. 21, no. 3, pp. 281–302, April 2003.

[15] B. Hamdaoui and K.G. Shin, "Characterization and analysis of multi-hop wireless MIMO network throughput," *in Proc. ACM Mobihoc*, pp. 120–129, Montréal, Québec, Canada, Sept. 2007.

[16] S. Haykin, D.J. Thomson, and J.H. Reed, "Spectrum sensing for cognitive radio," *Proc. IEEE*, vol. 97, no. 5, pp. 849–877, May 2009.

[17] S. Haykin, "Cognitive radio: Brain-empowered wireless communications," *IEEE Journal on Selected Areas in Communications*, vol. 23, no. 2, pp. 201–220, Feb. 2005.

[18] Y.T. Hou, Y. Shi, and H.D. Sherali, "Multicast communications in ad hoc network using directional antennas: A lifetime-centric approach," *IEEE Transactions on Vehicular Technology*, vol. 56, no. 3, pp. 1333–1344, May 2007.

[19] Y.T. Hou, Y. Shi, and H.D. Sherali, "Spectrum sharing for multi-hop networking with cognitive radio," *IEEE Journal on Selected Areas in Communications*, vol. 26, no. 1, pp. 146–155, Jan. 2008.

[20] Joint Tactical Radio System, http://www.globalsecurity.org/military/systems/ground/jtrs.htm/.

[21] *IEEE Journal on Selected Areas in Communications – Special Issue on MIMO Systems and Applications: Field Experience, Practical Aspects, Limitations and Challenges*, Guest Editors: M. Shafi, H. Huang, A. Hottinen, P.J. Smith, and R.A. Valenzuela, vol. 26, no. 6, Aug. 2008.

[22] *IEEE Journal on Selected Areas in Communications – Special Issue on Optimization of MIMO Transceivers for Realistic Communication Networks: Challenges and Opportunities*, Guest Editors: D. Palomar, T. Davidson, S. Barbarossa, A. Goldsmith, and G. Giannakis, vol. 25, no. 7, Sept. 2007.

[23] Y.-T. Kim, H. Lee, S. Park, and I. Lee, "Optimal precoding for orthogonalized spatial multiplexing in closed-loop MIMO systems," *IEEE Journal on Selected Areas in Communications*, vol. 26, no. 8, pp. 1556–1566, Oct. 2008.

[24] S-J. Kim, X. Wang, and M. Madihian, "Cross-layer design of wireless multihop backhaul networks with multiantenna beamforming," *IEEE Trans. on Mobile Computing*, vol. 6, no. 11, pp. 1259–1269, Nov. 2007.

[25] M. Kodialam and T. Nandagopal, "Characterizing the capacity region in multi-radio multi-channel wireless mesh networks," *in Proc. ACM Mobicom*, pp. 73–87, Cologne, Germany, Aug.–Sept. 2005.

[26] P. Kyasanur and N.H. Vaidya, "Capacity of multi-channel wireless networks: Impact of number of channels and interfaces," *in Proc. ACM Mobicom*, pp. 43–57, Cologne, Germany, Aug.–Sept. 2005.

[27] X-Y. Li and Y. Wu, "Maximizing throughput multicast routing for wireless networks," *in Proc. IEEE International Conf. on Wireless Algorithms, Systems and Applications*, pp. 3–10, Chicago, IL, Aug. 2007.

[28] W. Liang and X. Guo, "Online multicasting for network capacity maximization in energy-constrainted ad hoc networks," *IEEE Trans. on Mobile Computing*, vol. 5, no. 9, pp. 1215–1227, Sept. 2006.

[29] X. Liu and W. Wang, "On the characteristics of spectrum-agile communication networks," *in Proc. IEEE DySpan*, pp. 214–223, Baltimore, MD, Nov. 2005.

[30] J. Ma, G.Y. Li, and B.H. Juang, "Signal processing in cognitive radio," *Proc. IEEE*, vol. 97, no. 5, pp. 805–823, May 2009.

[31] J.E. Mitchell, "Branch-and-cut algorithms for combinatorial optimization problems," *Handbook of Applied Optimization*, pp. 65–77, Oxford University Press, Jan. 2002.

[32] J. Mitola, "Cognitive radio architecture evolution," *Proc. IEEE*, vol. 97, no. 4, pp. 626–641, April 2009.

[33] H.L. Nguyen and U.T. Nguyen, "Channel assignment for multicast in multi-channel multi-radio wireless mesh networks," *Wireless Communications and Mobile Computing*, vol. 9, no. 4, pp. 557-571, April 2009.

[34] A. Orda and B.-A. Yassour, "Maximum-lifetime routing algorithms for networks with omnidirectional and directional antennas", *in Proc. ACM Mobihoc*, pp. 426–437, Urbana-Champaign, IL, May 2005.

[35] J.M. Peha, "Sharing spectrum through spectrum policy reform and cognitive radio," *Proc. IEEE*, vol. 97, no. 4, pp. 708–719, April 2009.

[36] A.S.Y. Poon, R.W. Brodersen, and D.N.C. Tse, "Degrees of freedom in multiple-antenna channels: A signal space approach," *IEEE Trans. on Information Theory,* vol. 51, no. 2, pp. 523–536, Feb. 2005.

[37] E.M. Royer and C.E. Perkins, "Multicast operation of the ad-hoc on-demand distance vector routing protocol," *in Proc. ACM Mobicom,* pp. 207–218, Seattle, WA, Aug. 1999.

[38] SAFECOM, http://www.safecomprogram.gov/SAFECOM/.

[39] P. Setoodeh and S. Haykin, "Robust transmit power control for cognitive radio," *Proc. IEEE,* vol. 97, no. 5, pp. 915–939, May 2009.

[40] M. Shenouda and T. Davidson, "A design framework for limited feedback MIMO systems with zero-forcing DFE," *IEEE Journal on Selected Areas in Communications,* vol. 26, no. 8, pp. 1578–1587, Oct. 2008.

[41] Y. Shi and Y.T. Hou, "Optimal power control for multi-hop software defined radio networks," *in Proc. IEEE Infocom,* pp. 1694–1702, Anchorage, AK, May 2007.

[42] K. Sundaresan, R. Sivakumar, M.A. Ingram, and T-Y Chang, "A fair medium access control protocol for ad-hoc networks with MIMO links," *in Proc. IEEE Infocom,* pp. 2559–2570, Hong Kong, China, March 2004.

[43] I.E. Telatar, "Capacity of multi-antenna gaussian channels," *European Trans. Telecomm.,* vol. 10, no. 6, pp. 585–596, Nov. 1999.

[44] M. Trivellato, F. Boccardi, and H. Huang, "On transceiver design and channel quantization for downlink multiuser MIMO systems with limited feedback," *IEEE Journal on Selected Areas in Communications,* vol. 26, no. 8, pp. 1494–1504, Oct. 2008.

[45] D. Tse and P. Viswanath, *Fundamentals of Wireless Communication,* Cambridge University Press, June 2005.

[46] Vanu Inc., http://www.vanu.com/.

[47] H. Viswanathan, S. Venkatesan, and H. Huang, "Downlink capacity evaluation of cellular networks with known-interference cancellation," *IEEE Journal on Selected Areas in Communications,* vol. 21, no. 5, pp. 802–811, June 2003.

[48] P-J. Wan, G. Calinescu, and C-W. Yi, "Minimum-power multicast routing in static ad hoc wireless networks," *IEEE/ACM Transaction on Networking,* vol. 12, no. 3, pp. 507–514, June 2004.

[49] B. Wang and S.K.S. Gupta, "G-REMiT: An algorithm for building energy efficient multicast trees in wireless ad hoc networks," *in Proc. IEEE Int. Symp. Netw. Comput. and Appl.,* pp. 265–272, Cambridge, MA, April 2003.

[50] J.E. Wieselthier, G.D. Nguyen, and A. Ephremides, “Algorithms for energy-efficient multicasting in static ad hoc wireless networks,” *ACM Mobile Networks and Applications (MONET)*, vol. 6, no. 3, pp. 251–263, June 2001.

[51] J.E. Wieselthier, G.D. Nguyen, and A. Ephremides, “On the construction of energy-efficient broadcast and multicast trees in wireless networks,” *in Proc. IEEE Infocom*, pp. 585–594, Tel Aviv, Israel, March 2000.

[52] A. Wyglinski, M. Nekovee, and Y.T. Hou, Editors, *Cognitive Radio Communications and Networks: Principles and Practice*, Elsevier, Dec. 2009, ISBN-13: 978-0-12-374715-0.

[53] G. Zeng, B. Wang, Y. Ding, L. Xiao, and M. Mutka, “Multicast algorithms for multi-channel wireless mesh networks,” *in Proc. IEEE ICNP*, pp. 1–10, Beijing, China, Oct. 2007.